Hydrological changes during the last millennium in three subarctic permafrost peatlands and their link to climate shifts

Faculty of Biological and Environmental Sciences

Department of Environmental Sciences

Environmental Change and Global Sustainability

University of Helsinki

Master's Thesis

Veronica Ahonen

February 2019

Tiedekunta - Fakultet - Faculty		Laitos - Institution - Department	
Bio- ja ympäristötieteellinen tiedekunta		Ympäristötieteiden laitos	
Tekijä - Författare - Author			
Veronica Ahonen			
Työn nimi - Arbetets titel - Title			
Hydrological changes during the last millennium in three subarctic permafrost peatlands and their link to climate shifts			
Oppiaine - Läroämne - Subject			
Environmental Change and Global Sustainability			
Työn laji/ Ohjaaja - Arbetets art - Level		**Aika - Datum - Month and year**	**Sivumäärä - Sidoantal - Number of pages**
Pro gradu -tutkielma		27.2.2019	64

Tiivistelmä - Referat - Abstract

Ikiroutasoilla on suuri hiilensidontakapasiteetti, jonka ansiosta ne ovat tärkeitä ilmaston säätelijöitä. Noin 14% planeettamme maaperän orgaanisesta hiilestä on varastoituneena subarktisen alueen ikiroutasoihin, jotka ovat herkkiä ilmastonmuutoksille pohjoisesta sijainnistaan johtuen. Ikiroutasuot toimivat myös elinympäristönä lukuisille kosteuden muutoksille herkille lajeille, kuten sammalille ja kuoriameboille. Näitä lajeja voidaan käyttää aikojen kuluessa tapahtuvien hydrologisten muutosten tutkimiseen, joka mahdollistaa tulevan ilmastoresponssin mallintamisen.

Tässä pro gradu -tutkielmassa tutkitaan hydrologian muutoksia kolmelta ikiroutasuolta pohjois-Ruotsin Taavavuomasta ja Abiskosta kerätyissä kairanäytteissä kuoriamebojen lajistokoostumusta apuna käyttäen. Lajistokoostumukset yhdistettiin radiohiili- (^{14}C) ja lyijyajoitusten (^{210}Pb) tuloksiin menneiden aikojen vedenpinnan korkeuden rekonstruoimiseksi. Tulokset ulottuivat neljän eri ilmastovaiheen ajalle. Rekonstruktioita verrattiin menneisiin kuoriameboista tehtyihin tutkimuksiin ymmärtääksemme, kuinka ikiroutasuot ja niiden lajisto reagoivat soiden aktiivisessa turvekerroksessa tapahtuviin hydrologian muutoksiin.

Kolmesta tutkimuskohteestamme vain Taavavuomasta kerätyt kairanäytteet ulottuivat niin kutsutulle Dark Age Cold Periodille sekä keskiajan lämpökaudelle. Molempien kairanäytteiden lajistokoostumukset viittasivat vedenpinnan vaihdelleen Dark Age Cold Periodin aikana, mutta keskiajan lämpökauden aikana tulokset olivat keskenään ristiriitaisia, toisen kohteista osoittaessa kosteampaan ja toisen kohteista kuivempaan keskiajan lämpökauteen. Tutkimustulokset viittaavat kosteampaan pieneen jääkauteen sekä kuivempaan teollistumisen jälkeiseen lämpökauteen kahdessa kolmesta kohteesta, tukien menneitä tutkimuksia. Yhdessä kohteessa tulokset olivat päinvastaisia.

Tulokset osoittavat kuoriamebakoostumuksen vaihdelleen runsaasti aikojen kuluessa. Tämä viittaa siihen, että soiden hydrologia voi vaihdella nopeasti ja huomattavan paljon jopa paikallistasolla. Kuoriamebojen huonosti tunnettu ekologia hankaloittaa tulosten tulkintaa, ja siksi erilaisten, toisiaan tukevien indikaattorien käyttäminen on välttämätöntä luotettavien tulevaisuuden ennusteiden tekemiseksi.

Ohjaaja tai ohjaajat – Handledare – Supervisor or supervisors

Minna Väliranta

Säilytyspaikka - Förvaringsställe - Where deposited

Ympäristötieteiden laitos, Helsingin yliopisto

Muita tietoja - Övriga uppgifter - Additional information

Tekijä - Författare - Author
Veronica Ahonen

Työn nimi - Arbetets titel - Title
Hydrological changes during the last millennium in three subarctic permafrost peatlands and their link to climate shifts

Oppiaine - Läroämne - Subject
Environmental Change and Global Sustainability

Tiivistelmä - Referat - Abstract

Permafrost peatlands have the capacity to store significant amounts of carbon, and thus they act as important controllers of the climate. Approximately 14% of the world's soil organic carbon pool is stored in permafrost peatlands, which are sensitive to climatic fluctuations due to their location in the high latitudes of the subarctic zone. Permafrost peatlands also act as a habitat for a large number of moisture-sensitive organisms, such as bryophytes and testate amoebae, which can be used to study how the hydrology of peatlands has changed and will continue to change throughout time, giving us an opportunity to predict the future of peatlands under a changing climate.

In this Master's Thesis I examined the testate amoebae composition and used these species as indicators to study hydrological fluctuations from three subarctic permafrost peatland cores extracted from Taavavuoma and Abisko in northern Sweden. The species compositions were combined with radiocarbon (^{14}C) and lead (^{210}Pb) dates to reconstruct the past water table levels for the late Holocene, spanning four climatic periods. The reconstructions were then compared to past studies on testate amoebae to understand how permafrost peatlands and their species assemblages respond to changes in the hydrology of the active layer of the peat.

Out of the study sites only the Taavavuoma cores spanned the Dark Age Cold Period (DACP) and Medieval Climate Anomaly (MCA). Species compositions in both cores indicated fluctuating water tables during the DACP, but during the MCA the results began to contradict with one site showing a wetter, and the other a drier MCA. Two out of three study sites indicated a wetter Little Ice Age and a drier Post-Industrial Warming, supporting past studies indicating similar results, whereas one study site gave opposite results.

The results indicated large variability in testate amoebae assemblages throughout time, indicating that the hydrology of peatlands can change very abruptly and vary considerably even on a local scale. Modelling is however complicated by the poorly known ecology of testate amoebae, which is why a multi-proxy approach is essential to reliably predict the future fate of permafrost peatlands.

Ohjaaja tai ohjaajat – Handledare – Supervisor or supervisors
Minna Väliranta

Säilytyspaikka - Förvaringsställe - Where deposited
Faculty of Environmental Sciences, University of Helsinki

Muita tietoja - Övriga uppgifter - Additional information

TABLE OF CONTENTS

1. Introduction

Peatlands are ecosystems dominated by peat forming plants such as sedges and mosses. Peat itself consists of dead organic matter with a maximum of 25% of inorganic matter as dry mass. Geologically a deposit can be defined as a peatland when the depth of peat is over 30 centimeters (Turunen et al. 2002). Peatland initiation can occur via paludification or lake infilling (Moore 1987). A majority, or 80% of peatlands are located in the northern high and temperate latitudes, and the remaining 20% in subtropics and tropics (Yu et al. 2010).

On northern latitude peatlands the cold climate, limited oxygen diffusion resulted from waterlogging, and inherent decomposition resistance in litter slow down the microbial processes. Due to this the annual net primary production and total energy fixation by gross photosynthesis (GP) of the vegetation generally exceed the ecosystem respiration (ER) and decomposition. In this case the gas balance or Net Ecosystem Exchange (NEE) is negative, leading into the accumulation of carbon instead of carbon loss to the atmosphere, making northern peatlands efficient carbon sinks (e.g. Moore 1987, Lai 2009, Lara et al. 2015).

In a course of time the accumulated peat will form two functionally different layers in the peat profile: the oxygen-rich surface layer called the acrotelm, which overlies the oxygen-poor peat layer, defined as the catotelm (Ingram 1978). The average annual water table depth defines the boundary of these two layers (Clymo 1984). The decomposition rate of the anaerobic layer is only 0.1% of the rate of the aerobic layer (Belyea & Clymo 1999).

Peatlands are generally classified into three types: fens, bogs and palsa or permafrost peatlands (Lai 2009). In general, the young peatland stages are fens, and as succession proceeds, they transform into bogs. Northernmost peatlands act as an exception, since old northern fens have not developed into bogs. However, the ultimate reason for their slow peat accumulation rate is poorly known (Moore 1987). The main distinctive factor between peatland types is surface topography, which influences both hydrology and the dominant vegetation type. In fens the center of the peatlands lies lower than the edges, allowing the influence of surface runoff and groundwater, leading into a higher level of eutrophy. Fens are dominated by herbs and sedges such as *Carex* and *Eriophorum,* and bryophytes such as brown mosses and fen Sphagna (Lai 2009).

In bogs, the peat accumulation over time creates a thick peat mound, resulting in a dome which receives its water and nutrients solely from precipitation (Siegel 1988). Bogs are generally more ombrotrophic and acidic than fens. Only few species thrive in such conditions, most importantly *Sphagnum* mosses such as *Sphagnum fuscum,* and dwarf ericaceous shrubs such as *Calluna vulgaris* and *Empetrum nigrum* (Lai 2009). Permafrost peatlands have the characteristics of both bogs and fens: high hummocks resemble bog conditions, while low lawns are dominated by fen vegetation (Lara et al. 2015).

Peatlands are dynamic ecosystems, which change in time due to internal and external forcing. When considering the impact of climate variation on peatland functioning, it is necessary to differentiate whether the historical forcing and consequent changes in peatland dynamics have been allogenic (external) or autogenic (internal). Allogenic forcing results from abiotic factors, such as post-fire succession or changes in climate. Autogenic forcing is resulted from biotic changes such as fluctuations in peat thickness and vegetation cover (Payette 1988).

Permafrost peatlands contain characteristics of several peatland types and comprehensive knowledge of hydrology dynamics and forcing mechanims have long remained unresolved. Reconstructing past hydroclimatic conditions and discerning between allogenic and autogenic processes preferably calls for a multi-proxy approach (Lamarre et al. 2012). However, testate amoebae have proven as a very suitable proxy to study changes in hydrology (e.g. Amesbury et al. 2016, Swindles et al. 2015b, Zhang et al. 2017), and acts as the main proxy applied in this thesis project.

1.1. Peatlands and carbon dynamics

Peatlands act as significant carbon sinks and sources (Korhola et al. 2010). They uptake and release atmospheric carbon in two forms: carbon dioxide (CO_2) and methane (CH_4). Their sink function is important, since they transfer carbon from the fast cycle (photosynthesis) to the long carbon cycle (peat formation). Peatland accumulation rates for carbon range from 20 to 100 grams of carbon m^{-2} yr^{-1} (Moore & Knowles 1989). During the post glacial period peatlands have worked as a net sink, sequestering approximately 76 Tg or 10^{12} tons of carbon yr^{-1} (Loisel et al. 2014). However, they also play a key role in carbon release: peatlands release 46 Tg of CH_4 into the atmosphere annually, which is equivalent to 12.2% of global methane emissions (Lai 2009). Thus, the development of boreal

wetlands is at least partly responsible for the global positive CH_4 increase after 5000 BP[1] (Korhola et al. 2010). The global warming potential of methane is 25 to 100, which means that one kilogram of methane equals 25 kilograms of carbon dioxide in a time span of 100 years (Boucher et al. 2009). Methane is thus a powerful, yet short-lived greenhouse gas, with a lifespan of only 12 years in contrast to carbon dioxide, which can remain in the atmosphere even for centuries (Canadell et al. 2007). The balance between carbon dioxide and methane release on a peatland is controlled mainly by temperature and hydrology. These in turn determine the species composition (Lai 2009).

Methane is generated in anaerobic conditions by methanogenic bacteria (Garcia et al. 2000). Due to this, methanogens thrive in environments with a high water table, such as fens and bog depressions. The carbon accumulation rate of fens is slower than that of bogs, which is why bogs act as net carbon sinks, and fens as net carbon sources (Lai 2009). Whether the once accumulated carbon is released as carbon dioxide or methane, is strongly linked to the depth of the water table. When the water table depth increases, the oxidized peat column thickens, which determines the ratio of aerobic and anaerobic decomposition (Moore & Knowles 1989).

Even though high latitude peatlands occupy less than 3% of global land area, they contain 30% of the world's soil organic carbon pool: during the Holocene period (past 11.500 years), peatlands have stored roughly 500 Gt of carbon (Loisel et al. 2014). Because of their important connection to the carbon cycle, high latitude peatlands have been integrally linked to both past and present changes in the climate (Fisher et al. 2011), and served as persistent long-term carbon sinks, accumulating on average 5 Gt of carbon per century (Yu et al. 2010).

1.2. Peatlands and the past climate

Peatlands have gone through several climate fluctuations during the Holocene due to natural forcing, such as orbital and solar variability and atmospheric carbon concentrations (Mayewski et al. 2004). There have been five major climatic periods during the Holocene: the Holocene Thermal Maximum or HTM from roughly 11000 to 5000 years BP (Renssen et al. 2012), the Roman Warm Period or RWP from 1-300 AD, the Dark Age Cold Period (DACP) from 300-800 AD, the Medieval Climate

---

[1] BP = before 1950 AD

Anomaly (MCA) from 800-1300 AD, the Little Ice Age (LIA) from 1300-1900 AD, and the current, post-industrial temperature increase thereafter (e.g. Broecker 2001, Ljunqvist 2010). The exact beginning and termination dates for these periods differ regionally (e.g. Renssen et al. 2009, Treat & Jones 2018), but are often inferred from historical peat proxy records and reflected as changes in vegetation types and / or rate of permafrost aggradation. Increases in fen vegetation generally coincide with wetter and warmer periods, whereas colder and drier periods in turn are linked to bog phases and permafrost aggradation (Oksanen & Väliranta 2006, Schuur et al. 2008).

Out of the past climate periods of the Holocene four are explored in this thesis: the Dark Age Cold Period, the Medieval Climate Anomaly, the Little Ice Age and post-industrial temperature increase.

Compared to the more well-studied Medieval Climate Anomaly and Little Ice Age, the climate of the Dark Age Cold Period is generally poorly understood (Helama et al. 2017). A review article by Helama et al. (2017) compiled 114 paleoclimate studies on the DACP and found that 55% of the studies suggested a cooling trend throughout the northern hemisphere during the DACP, 20% of studies suggested that this cooling was linked to hydroclimatic conditions, with 11% of those studies presenting wet or moist conditions. Yet some Fennoscandian proxies suggest a dry pre-MCA period overlapping with the DACP (Ljungqvist 2010, Linderholm et al. 2018). The variation in the results suggests that this was a period of an unstable climate, possibly caused by a combination of changes in solar activity, negative NAO phase and a series of large volcanic eruptions (Helama et al. 2017).

The Medieval Climate Anomaly has been regarded as a warmer period between the DACP and the LIA. Previous studies with testate amoebae (e.g Väliranta et al. 2012) and tree ring data (e.g Cook et al. 2015) indicate dry conditions in this period. The new synthesis compiled by Linderholm et al. (2018) also suggests a drying during the MCA, until the abrupt wet conditions in early LIA.

The Little Ice Age or LIA was a period of cooler climates from 1300 to 1900 AD. The LIA coincides with lower summer insolation in the northern hemisphere due to several volcanic eruptions, orbital forcing and minimal sunspot activity during the period called the Maunder Minimum (1645-1715 AD) when almost no sunspots were visible (Ribes & Nesme-Ribes 1993). After this period the increase in the atmospheric CH_4, CO_2 and N_2O concentrations is associated with a 0.3 ° C rise in global temperature. In addition to industry, deforestation and draining of wetlands have played an

important role in both biophysical and biogeochemical climate feedbacks. Deforestation has led to the overall decrease in the amount of terrestrial carbon sinks. Wetland draining has increased surface dryness, and the lowering of the water table has led to heightened CO_2 emissions, but due to the simultaneous decrease in CH_4 emissions the net effect has been positive (Wanner et al. 2008). Generally, the climate of the past few centuries has been dry, with a trend towards wetter conditions in the past decades (Zhang et al. 2018).

1.3. Permafrost peatlands

Permafrost occurs where the ground temperature remains below or at 0 ˚C for at least two subsequent years. Depending on the spatial coverage of frozen ground, permafrost can be defined as continuous (91-100%), discontinuous (51-90%), sporadic (10-50%) or isolated (<10%) permafrost (Tarnocai et al. 2009). In total, permafrost covers 25% of the land surface in the northern hemisphere, where the mean annual ground temperature remains below zero.
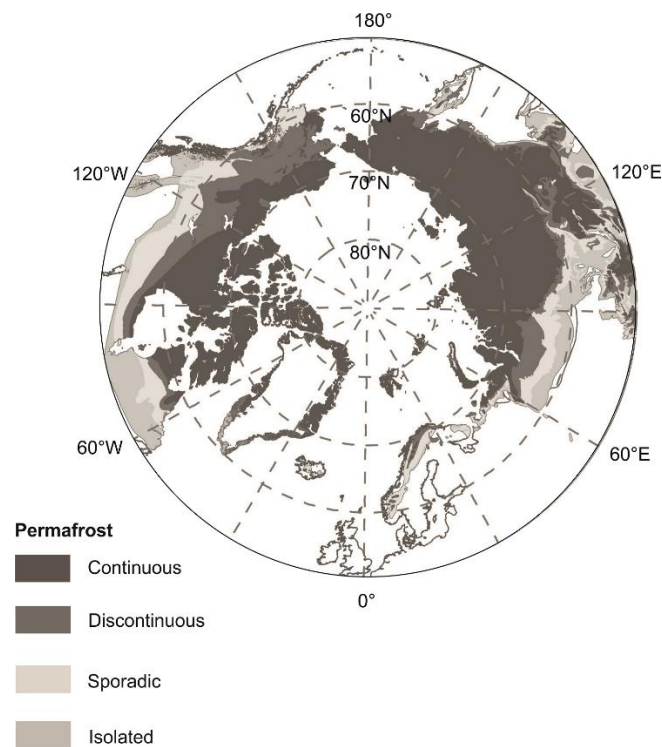

Figure 1. Map of permafrost occurrence in the Arctic. Edited from Brown et al. (1997).

The development of permafrost peatlands began in Fennoscandia roughly 2500 years ago (e.g. Oksanen & Väliranta 2006, Treat & Jones 2018) during a period of drier and cooler conditions following the Holocene Thermal Maximum (Holmquist et al. 2016). A decrease in summer insolation across northern latitutes led to an increase in permafrost aggaradation and a shift from wet fens to dry bogs and permafrost peatlands. A peak in permafrost aggradation occurred from 1200 – 1950 AD, which coincides roughly with the Little Ice Age. Coolest temperatures of the LIA occurred 1750 AD and the maximum extent of permafrost was probably reached 1825 AD (Treat & Jones 2018). Permafrost peat development studies have revealed that some permafrost peatlands were formed during cold conditions of the LIA, while significantly older permafrost formations have been dated also to the warm conditions of the Medieval Climate Anomaly (Borge et al. 2017).

In Fennoscandia, permafrost peatlands represent the southern- and westernmost extents of discontinuous permafrost (Borge et al. 2017). Since the mean air and ground temperatures are too high for sustained permafrost, the distribution and extent of permafrost is determined by local hydrology, topography, vegetation and precipitation (Schuur et al. 2008). Due to the insulating properties of peat, especially *Sphagnum* (Kokfelt et al. 2009), permafrost may exist in regions where the mean annual air temperature is as warm as 1 or 1.5 ˚ C (Camill 2005). However, the narrow climatic range in which permafrost peatlands currently occur makes them sensitive to climate variability. The most severe effect is caused by increased winter warming, which prohibits the formation of new permafrost, further accelerated by fast spring thaw (e.g. Seppälä 1997, Camill 2005). Increase in snowfall results in a thicker insulating snow cover inhibiting formation and / or maintaining of ice core (Zhang 2005).

Permafrost thaw causes conversion of ombrotrophic permafrost palsa mounds into more minerotrophic wet fen habitats (Swindles et al. 2015a). When permafrost melts, the carbon storage which was previously frozen becomes available for microbial processes, which leads into altered vegetation composition and ecosystem productivity (Olefeldt & Roulet 2012). The degradation rate of permafrost formations depends on their size, with smaller palsa domes degrading significantly faster than large peat plateaus (Oksanen & Väliranta 2017). Their dome-like shape also makes them vulnerable to block erosion (Borge et al. 2017).

Permafrost peatlands store 14% of the global soil carbon (Hugelius et al. 2014). Permafrost thaw has increased drastically during the past 150 years and will most likely increase further in the future (Luoto & Seppälä 2002, Schuur et al. 2008). Even in the least extreme warming scenario of 2 °C degrees, the amount of permafrost may be reduced by 25%, which would lead to the release of up to 100 Pg of carbon during the next 100 years (Canadell et al. 2007). Permafrost peatlands contain substantial amounts of dissolved organic carbon, which may be mobilized into aquatic environments or mineralized to CO_2 and CH_4, which are eventually lost into the atmosphere (Kokfelt et al. 2009).

According to Swindles et al. (2015a), there are five distinct phases of permafrost degradation. In Phase 1, the permafrost peatlands are pristine and permafrost remains intact. In Phase 2 the gradual drying of the surface peat lowers the water table. The oxidation of the surface peat leads into increased aerobic decomposition and evaporation. At this phase the peatlands act still as carbon sinks, but CO^2 release has risen due to increased cellular respiration of plants and microbes. Once these changes have taken place, the peatland enters Phase 3. The positive feedbacks will cause rapid shrinkage of dried peat, which results in the cracking and collapsing of permafrost domes. In Phase 4, the thaw water released from melted permafrost starts saturating into the collapsed peat domes. Phase 5 is permafrost-free Arctic fen. The peatland surface is flat and fed by surface and groundwater flow from adjacent areas. The high water table leads into anoxic conditions throughout the peat layer, resulting in an elevated flux of CH_4. However, the wetness and eutrophy also increase productivity, leading into the rapid accumulation of peat. Thus, collapsed permafrost peatlands may have the potential to sequester carbon in the future (Swindles et al. 2015a).

1.4.   Peatlands and climate change

Current global warming estimates indicate that the Arctic regions will experience greater temperature increases than any other areas on the globe. The worst scenario is an up to 8.3 ± 1.9 ° C increase during the following century, or the RCP8.5 scenario, whereas the global increase is on average only 3.7 ± 0.7 ° C (Collins et al. 2013). This phenomenon is called the *Arctic Amplification*, which is a result of positive feedbacks caused by the decreased area of snow and ice cover (Screen & Simmons, 2010). As white snow and ice surfaces melt, their albedo or ability to reflect radiation is reduced, leading into increased absorption of solar insolation (Serreze & Francis 2006). This in turn increases atmospheric humidity and a positive warming feedback, because water vapor is the most powerful

greenhouse gas (Screen & Simmons 2010). Overall, the modern world is 1.0 degrees warmer than during the pre-industrial period (IPCC 2018).

The hydrology and microhabitat conditions of peatlands will likely be severely affected. Although it is certain that peatlands have previously had a net cooling effect, their future fate remains uncertain (Collins et al. 2013). Peatlands have accumulated a significant carbon storage over the past thousands of years (Loisel et al. 2014, Lara et al. 2015). The two main global warming scenarios are the warmer/wetter scenario and the warmer/drier scenario. Both scenarios expect rising temperature, but in the former evapotranspiration rate remains positive, whereas in the latter it will decrease (Wu & Roulet 2014). Global warming threatens to accelerate the release of this carbon back to the atmosphere, further increasing global warming through a set of positive feedback loops described above (Fisher et al. 2011). Future scenarios suggest that peatlands will remain as carbon sinks at least until the end of the 21st century, but their carbon sink function will decrease with warming, switching their warming feedback from negative to positive (Gallego-Sala et al. 2018). However, permafrost thaw is a slow process, and thus is has been estimated that complete melt of permafrost plateaus will take 175-260 years (Borge et al. 2017).

1.5. Testate amoebae

Testate amoebae are a polyphyletic group of shelled Protozoa common to wetlands. They are small unicellular Protists with a size ranging from 20-200 μm. One gram of dried peat can contain up to 10^4 individuals, and over 2000 species have been identified so far (Warner 1990). These predatory organisms are the most dominant group of Protozoa in Sphagnum mosses, which highlights their importance in the food chain of bacteria and fungi and the soil nutrient cycle (Mitchell et al. 2008). Testate amoebae account up to 30% of microbial biomass in soil (Charman et al. 2000).

Testate amoebae are commonly used proxies in addition to plant microfossils in predicting hydrological changes under a changing climate (e.g. Woodland et al. 1998, Charman et al. 2007, Väliranta et al. 2012, Zhang et al. 2017). Testate amoebae build a decay-resistant shell called a *test* from proteinaceous, calcareous or siliceous material that may contain organic or mineral particles from the surrounding environment. Abiotic and biotic factors such as food source, temperature and light affect the shell morphology, which results in a high degree of morphological variability both

among and within populations (Mitchell et al. 2008). Their tests are taxonomically distinctive and abundant in Holocene peats (Booth et al. 2010).

Figure 2. Diversity of testate amoebae. From left to right: *Euglypha tuberculata, Nebela wailesi* type, *Difflugia sp., Arcella catinus, Archerella flavum.* © Veronica Ahonen.

The main controller of the community species composition is the moisture content of the contemporary surface peat (Booth et al. 2010). Testate amoebae can be roughly grouped according to their *water table optimum* on a scale from wet to dry (e.g. Swindles et al. 2015b, Zhang et al. 2018). Those species that do not respond strongly to water table fluctuations and appear in all conditions are labeled as generalists (Charman et al. 2007). Many taxa have clear water table optimas. One of these taxons are the *Difflugia,* which thrive in wet conditions due to their tests for which they use silica particles (Mitchell et al. 2008). In drier conditions, test shape is important. Mitchell et al. (2008) argue that thin tests are better suited to life in thin water films under drier conditions, one example is *Trigonopyxis spp*. Some species, such as *Cyclopyxis arcelloides, Hyalosphenia papilio* and *Nebela tincta* have wider tolerance ranges than others and can thrive widely along the hydrological gradient (Mitchell et al. 2008, Tolonen et al. 1992). In general, dry taxa are less sensitive to changes in moisture conditions than wet taxa, which may have very narrow tolerance ranges (Charman et al. 2007, Zhang et al. 2017).

Table 1. An example of a hydrological classification, according to the training set by Swindles et al. 2015b.

Wet	**Wet-intermediate**	**Intermediate**	**Dry**	**Generalist**
Arcella discoides	*Archerella flavum*	*Nebela militaris*	*Arcella catinus* type	*Assulina muscorum*
Centropyxis aculeate	*Hyalosphenia papilio*	*Nebela tincta*	*Trigonopyxis sp.*	*Euglypha sp.*
Difflugia sp.	*Placocista spinosa*			

The most recent studies of testate amoebae in Scandinavian subarctic region is the study by Zhang et al. (2017), which combines testate amoebae into a new training set, classifying testate amoebae according to their water table depth optimum and tolerance ranges.

Table 2. Testate amoebae water table optimas, modified from Zhang et al. (2017). Optimum: optimal water table *depth* (cm). Tolerance: water table *range* (cm). Narrow tolerance range <10, medium >10, wide >20. Class: hydrological classification. Wet optimum depth <10, intermediate >10, dry >20.

Family	Species	Optimum	Class	Tolerance
Assulina	*A. muscorum*	25	Dry	Wide
	A. seminulum	23	Dry	Wide
Archerella	*A. flavum*	10	Wet-intermediate	Medium
Arcella	*A. catinus* type	17	Intermediate	Medium
Cyclopyxis	*C. arcelloides* type	10	Wet-intermediate	Wide
Difflugia	*D. lucida*	3	Wet	Narrow
	D. pulex	8	Wet	Wide
	D. pristis	17	Intermediate	Medium
Euglypha	*E. spinosa* type	18	Intermediate	Wide
	E. tuberculata type	22	Dry	Wide
Hyalosphenia	*H. papilio*	8	Wet	Medium
	H. minuta	27	Dry	Wide
Nebela	*N. militars* type	16	Intermediate	Medium
	N. tincta type	12	Intermediate	Medium
Placocista	*P. spinosa*	8	Wet	Medium
Pseudodifflugia	*P. fascicularis*	11	Intermediate	Wide
	P. fulva	17	Intermediate	Medium
Trigonopyxis	*T. arcula* type	26	Dry	Medium
	T. minuta type	27	Dry	Medium

Testate amoebae can also be classified via their primary energy source into *mixotrophic* and *heterotrophic* (Jassey et al. 2013). The former have the capability to fix inorganic carbon through photosynthesis, when the latter only assimilate organic carbon through predation. Mixotrophic species such as *Archerella flavum* and *Hyalosphenia papilio* have been reported to respond negatively to increases in temperature and dryness; this further increases sensitivity of these species to environmental change (e.g. Jassey et al. 2015, Lamentowicz et al. 2015). Overall, the ecology of testate amoebae is still relatively poorly understood, and requires further study (e.g. Swindles et al. 2015b, Amesbury et al. 2016, Zhang et al. 2017).

1.6. Research aim and study background

This Master's thesis was conducted as a part of a larger research project funded by the Academy of Finland and carried out at the Environmental Change Research Unit (ECRU). The overall aim of the project is to study past, present and future climate-induced changes in Arctic permafrost peatlands as reflected in hydrology, vegetation, microbial composition and carbon dynamics. The increasing threat of global warming and its link to permafrost thaw and the so far limited knowledge of permafrost peatland biological and peat property dynamics motivate the study. The project compiles plant macrofossil, testate amoebae and geochemical analysis data to reconstruct paleohydrological conditions and carbon accumulation. My part of the project is to focus on the past changes in moisture conditions by applying testate amoebae communities as a proxy. The focus time period is the past millennium and the data were collected from three subarctic permafrost peatlands in northern Sweden. The leader of the project is docent Minna Väliranta. The other team members are doctoral student Sanna Piilo and Master student Ronja Hyppölä, whose thesis focuses on plant composition variations. PhD Hui Zhang and senior scientist Matt Amesbury provided help in the identification of testate amoebae.

Although permafrost peatland development and carbon accumulation (Treat & Jones 2018 and references therein) has been relatively actively studied, only few high-resolution studies on testate amoebae exist to accurately reconstruct past hydrological conditions (e.g. Swindles et al. 2015b, Amesbury et al. 2016, Zhang et al. 2017). This thesis aims to fill in the gaps.

My research hypotheses are:
1. *In peat records cold and warm periods can be observed via changes in moisture conditions, with warm periods commonly corresponding with dry and cold periods with wet conditions.*
2. *"The present is the key to understand the past" - Arctic peat layers contain moisture sensitive testate amoebae which allow the reconstruction of past climatic events.*

My research questions are:
1. *What kind of changes the testate amoebae compositions have experienced in the past?*

2. *Are the newly-reconstructed changes in hydrology comparable to previous climate reconstructions?*

2. Material and methods

2.1. Study sites

This study was conducted on two study sites in northern Sweden, Taavavuoma and Abisko, which are located in the discontinuous permafrost zone (Brown et al. 1997). The areas consist of frost-heaved, dry ombrotrophic hummocks and plateaus or palsas, surrounded by wet depressions and minerotrophic areas (Kokfelt et al. 2009). Both regions have experienced rapid warming and permafrost thaw during the twentieth century (Åkerman & Johansson 2018, http://www.helsinki.fi/kilpis/Ilmasto/tunnuslukuja.htm). Since the turn of the millennium, the mean annual temperature has consecutively exceeded 0 ˚ C, which is the threshold after which year-round permafrost can no longer be sustained. The annual rising temperature has led to the deepening of the active layer and the increase in surface wetness through the thawing of permafrost, which can be noticed as collapsed peat plateaus, palsas, and thermokarst lakes (e.g. Åkerman & Johansson 2008, Swindles et al. 2015a).

Several instrumental measurements have been conducted in the Abisko region (e.g Åkerman & Johansson 2008, Kokfelt et al. 2009, Swindels et al. 2015b). The climate of Abisko is drier and milder than other locations at similar latitudes, due to its position in the rain shadow of the Norwegian mountains and proximity to the Atlantic and thus the Gulf Stream (Åkerman & Johansson 2008). This results in a high influence of precipitation (Kokfelt et al. 2009), which varies considerably between seasons, the seasonal mean being 46 mm during spring and 136 mm during summer. Temperature varies between a winter mean of -9.3 ° C and a summer mean of 10.1 ° C (Åkerman & Johansson 2008).

Considerably less measurements have been carried out at the Taavavuoma region on temperature and precipitation. The closest weather station with a consecutive and reliable data record is Kilpisjärvi station at 69°03'N, 20°50'E approximately 60 kilometers north. At Kilpisjärvi the temperature varies

between a winter mean of -12,7 ° C and a summer mean of +9.3 ° C. Precipitation varies from a winter mean of 42,5 mm and a summer mean of 58 mm (http://www.helsinki.fi/kilpis/Ilmasto/tunnuslukuja.htm). Comparing the temperatures and precipitation regimes of Kilpisjärvi and Abisko, the mean temperature varies ±2.6 degrees, and precipitation as much as 78 mm, which makes the climate of Abisko considerably more oceanic than that of Kilpisjärvi and Taavavuoma.

Figure 3. Map of the study sites.
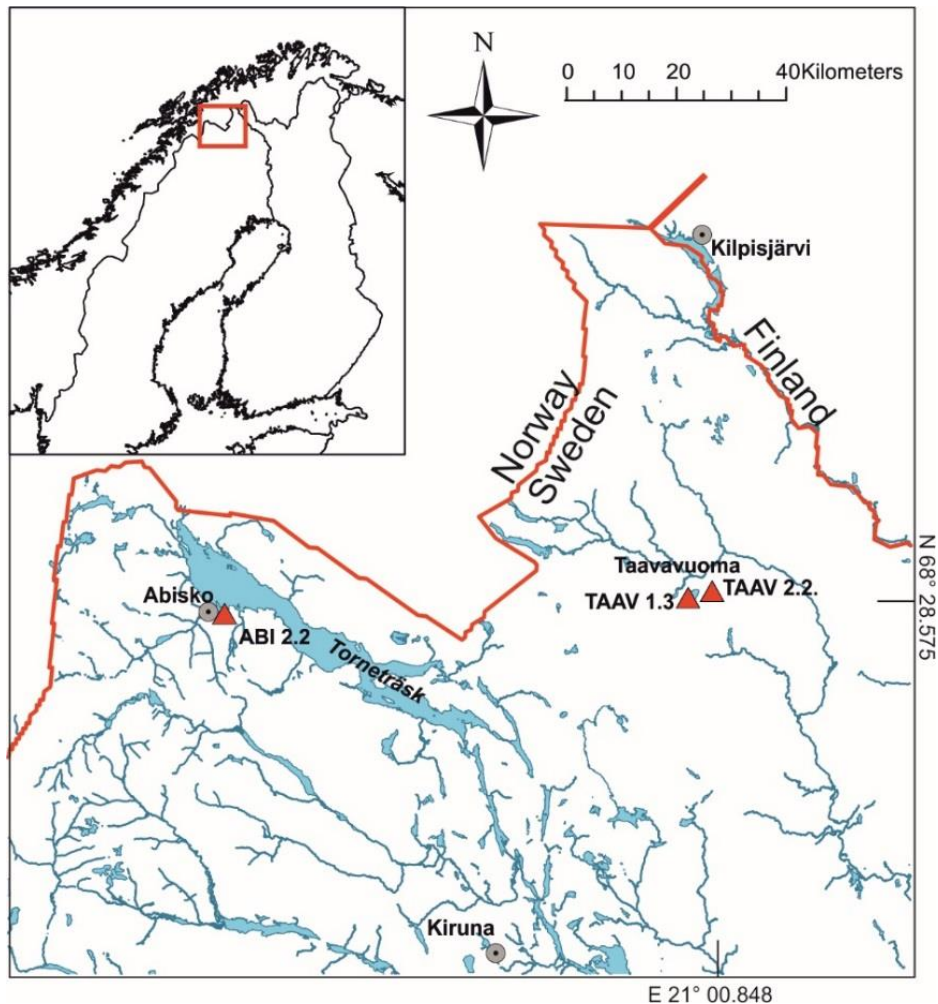
Two adjacent peatlands were cored in Taavavuoma and one peatland in Abisko. The first Taavavuoma coring site (Taav 1.3) was located at 68°28'N, 20°54'E west of the lake Dávvajávri at 661 meters from sea level. The second site (Taav 2.2) was located at 68°28.5'N, 21°01'E roughly 10 kilometers northeast at 554 meters from sea level. Dominant vegetation at both sites consisted of

Lichenes spp., Rubus chamaemorus, Sphagnum spp., and *Andromeda polifolia* at the Taav 1.3 coring site, and *Betula nana* at the Taav 2.2 coring site.

The Abisko core (Abi 2.2) was extracted south of Lake Torneträsk at 68°21'N, 18°52'E, situated 349 meters from sea level. A much higher abundance of vegetation was recorded, including *Andromeda polifolia, Betula nana, Dicranum spp., Empetrum nigrum, Eriophorum vaginatum, Lichenes spp., Polytrichum spp., Rubus chamaemorus, Sphagnum spp.* and *Vaccinium uliginosum.*

Figure 4. Coring sites for Abi 2.2 (left) and Taav 2.2 (right) cores. Photographs © Sanna Piilo.

2.2. Sample collection

The sample collection was performed on the 22-27 of August 2017 firstly in Taavavuoma and then Abisko. Two peatlands were cored from both study sites and three peat sections were extracted from

each peatland, i.e. 12 peat cores in total, of which I analyzed three samples: Abi 2.2, Taav 2.2 and Taav 1.3. The samples were taken from palsa surfaces with a *Sphagnum fuscum* coverage using a 60 cm x 7 cm x 5 cm aluminum peat box corer. After extraction the sample was photographed and the composition was described and marked down with 1 cm resolution. Each sample was packed in plastic, labeled and secured with duct tape, and placed inside a plastic gutter for transportation. The pH and water table depths for each coring site were measured and dominant vegetation was described.

Figure 5. Freshly extracted Taav 1.3 core. Table describing peat properties below:

Depth	**Peat properties**
0-3 cm	Fresh *Sphagnum*
3-10 cm	Dark peat with roots
10-15 cm	Light *Sphagnum* peat
15-20 cm	Well humified brown *Carex* peat
20-28 cm	Dark brown humified *Carex* peat
28-40 cm	Black humified peat
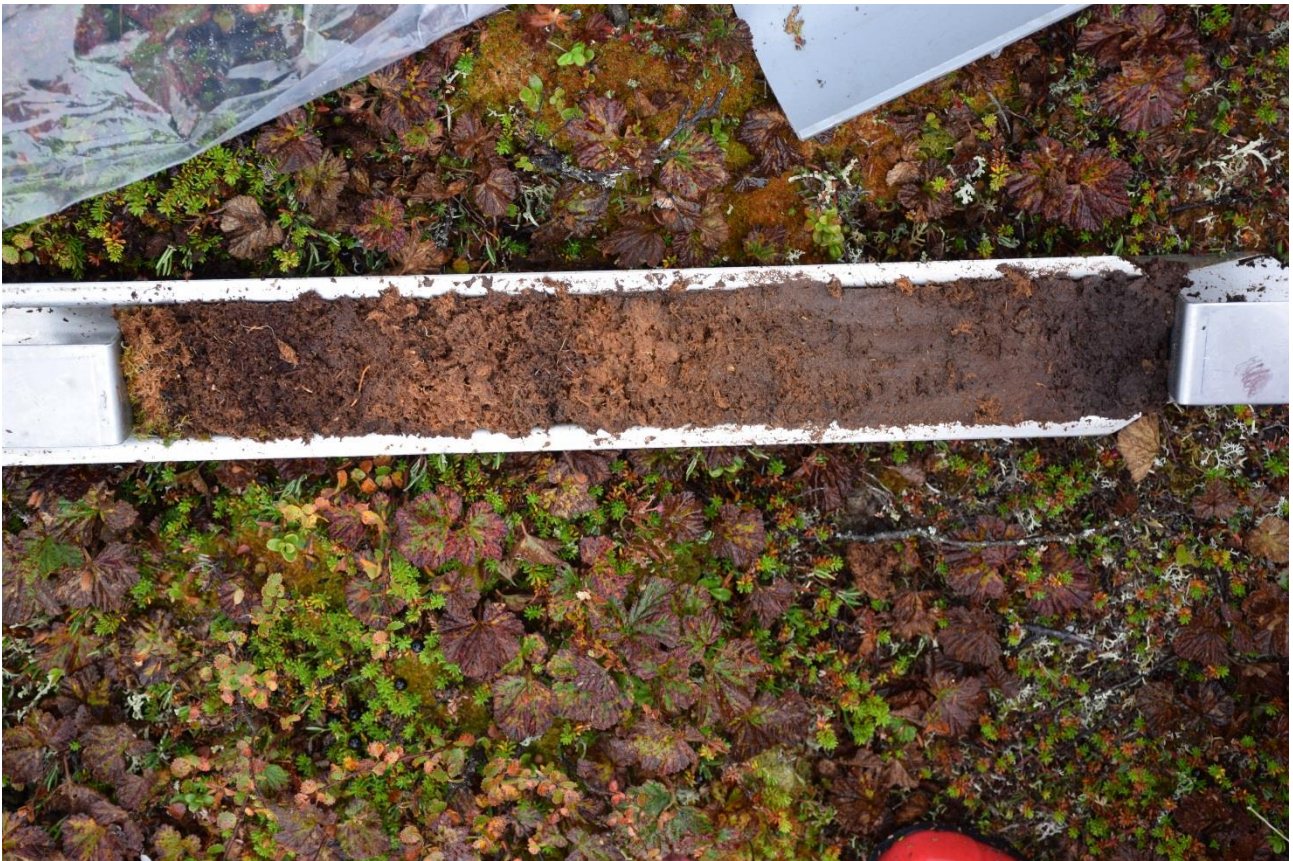
Figure 6. Freshly extracted Taav 2.2 core. Table describing properties below:

Depth	**Peat properties**
0-2 cm	Fresh *Sphagnum*
2-6 cm	Humified *Sphagnum* with roots
6-8 cm	Dark peat with roots
8-13 cm	Middle brown, humified mixed peat
13-19 cm	Light *Sphagnum* peat
19-21 cm	Dark mixed peat
21-27 cm	*Sphagnum* peat
27-32 cm	Humified mixed peat with *Sphagnum*
32-44 cm	Evenly humified brown *Carex* peat
44-50 cm	Black humified peat

Figure 7. Freshly extracted Abi 2.2 core. Table describing properties below:

Depth	Peat properties
0-7 cm	Fresh *Sphagnum*
7-17 cm	Dark peat with roots
17-21 cm	Transition zone between darker and lighter *Sphagnum peat*
21-27 cm	Light *Sphagnum* peat
27-40 cm	Dark mixed peat

The contemporary water table depths for the sampling sites were 20 cm at Taav 1.3, 22 cm at Taav 2.2 and 13 cm at Abi 2.2. pH was 5 for both Taavavuoma sites and 4.5 for the Abi 2.2 site.

2.3. Sample analysis

Each core sample was sliced in 1 cm subsamples that were packed in separately labeled Mini grip bags, labeled as Abi and Taav. To avoid contamination, rubber gloves were used and supplies were washed after each cut. The bags for each sample were then stored at 6 ° C until further analysis.

2.3.1. Testate analysis

Testate amoebae acted as the primary proxy for this study. They are routinely used as indicators of past change in peatland hydrology due to their quick response to environmental change. The species abundance-based reconstructed water table depths can be compared to instrumental and proxy-based climate records from the past few centuries (Booth et al. 2010). For analysis of testate amoebae samples, a modified version of the standard method by Booth et al. (2010) was applied. A subsample of known volume (measured via the Archimedes principle) was placed in a 250 ml beaker with distilled water and a clean stirring rod. One tablet of Lycopodium (batch # 938934) was added as an exotic marker. The samples were boiled for ten minutes and stirred occasionally, which helped to disaggregate the peat and disperse the spores. After boiling, the material was sieved through a 300-μm sieve and back-sieved with a 15- μm sieve, for coarse and small particulate matter. If the sample contained a high amount of plant debris, a 180 μm sieve was used instead of 300 μm- sieve. The matter from the 15- μm sieve was collected into a 50 ml centrifuge tube. The samples were centrifuged at 3000 rpm for five minutes in batches of four to retain the centrifuge balance. After centrifugation the samples were poured into 5 ml containers and stored at fridge temperature (Booth et al. 2010).

Sampling was conducted until the depth of 20 centimeters. This was due to time constraint and the fact that testates begin to decay as depth increases (Charman et al. 2000). However, in the case of the sample being still abundant in the depth of 20 cm, the sampling was continued until it became difficult or impossible to reach the minimum count of 50 specimen (Payne & Mitchell 2009), or the testates reached a depth that was considered sufficient (in this thesis, 29 centimeters was chosen).

The taxa were then identified to species or "type" level and calculated under a 400 x zoom light microscope with the help of Charman et al. (2000) and Sullivan & Booth (2007). The identification resolution was 2 centimeters, and a minimum of 100 specimen were calculated from each sample, although in some cases this count was exceeded due to the high abundance of testates. Count of 100 individuals is considered to be sufficient for most samples, although for deeper, highly decomposed samples 50 specimen are often counted (e.g. Payne & Mitchell 2009, Booth et al. 2010). In addition to testate amoebae the amount of Lycopodium spores was counted.
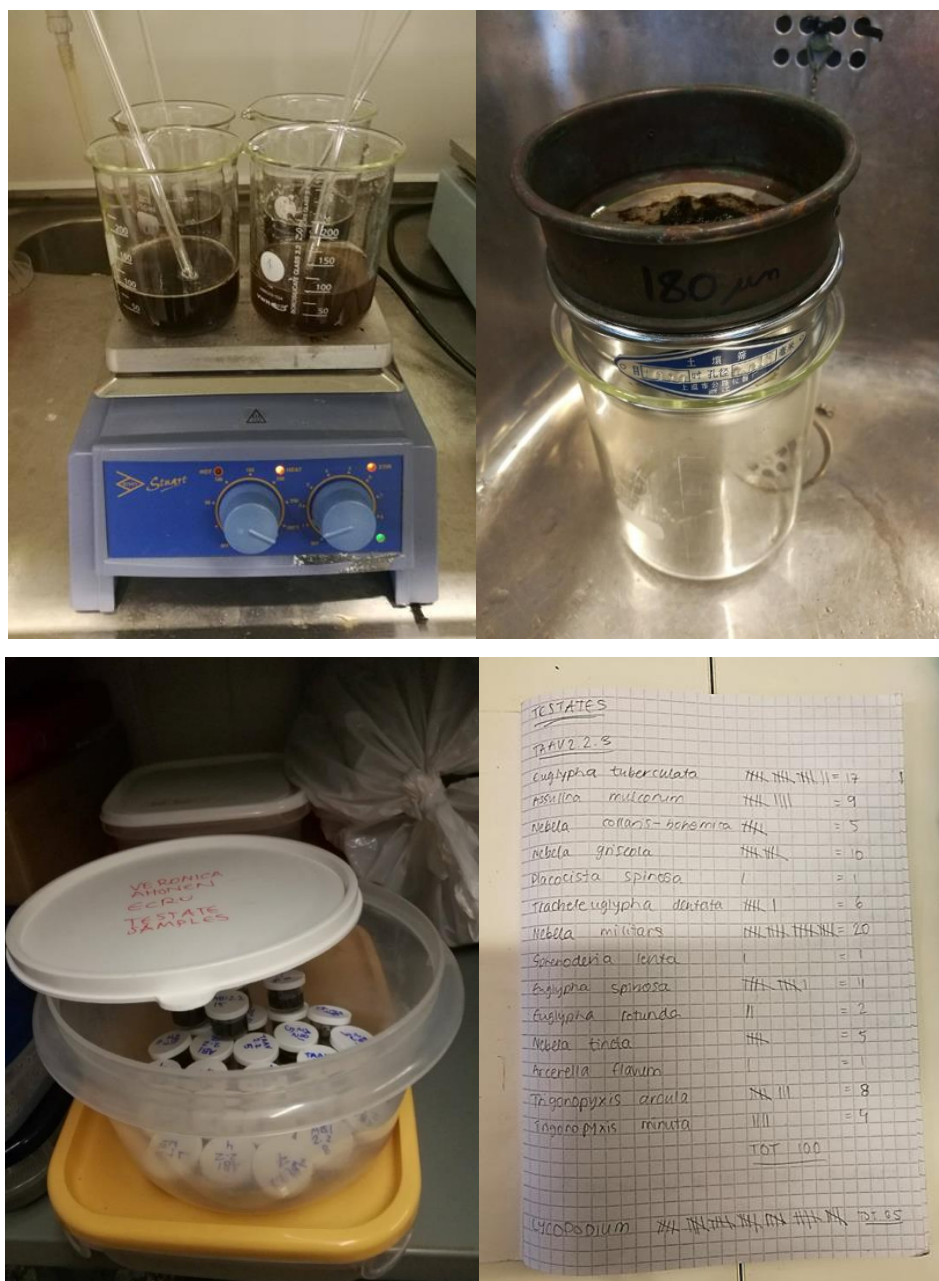
Figure 8. Preparation of testate samples. Top right: boiling of samples. Top left: 180 μm sieve on top and 15- μm back-sieve on bottom. Bottom right: prepared and labeled 5 ml testate sample containers in cold storage. Bottom left: notes of calculated specimen and Lycopodium in the Taav 2.2.3 sample.

2.3.2. Radiocarbon and lead dating

The peat samples for this thesis were dated via two traditional dating techniques: radiocarbon ^{14}C and lead ^{210}Pb dating. Radiocarbon dating is based on measuring the amount of radioactive carbon in an organism, using the ^{14}C isotope. This radioactive isotope is produced in the stratosphere, when cosmic

rays react with ^{14}N atoms. The resulting ^{14}C is oxidized into ^{14}CO$_2$, which mixes into the troposphere and becomes a part of the atmospheric CO$_2$ reservoir, and eventually enters the food chain via plant photosynthesis. Upon the death of an organism the uptake of fresh ^{14}C ceases, and the carbon goes through radioactive beta particle decay (Appleby & Oldfield 1978). The abundance of ^{14}C in an organism decreases by 1% every 83 years, such that after 5730 ± 40 years, only half of the original atoms remain (Godwin 1962). The calculated dates are announced in years before present (BP), where zero year is defined as 1950 Anno Domini. This is why younger layers are dated by other methods, often via ^{210}Pb (Turetsky et al. 2000).

For this study the radiocarbon amounts were measured via *accelerator mass spectrometry* or *AMS*. Subsamples for the radiocarbon analysis were taken inside the peat column to avoid modern carbon contamination. Samples were freeze-dried and later analyzed at the A.E Lalonde AMS Laboratory in Montreal, Canada by Sanna Piilo. For radiocarbon dating two dates were taken for each core: one from the bottom segment and one from the mid core. Radiocarbon BP ages were calibrated with the Calib 7.1 program, using the IntCal 13 calibration curve (Stuiver & Reimer 1993). Calibrated ages presented in this thesis are the mean values of the two Sigma range rounded to the nearest 5.

Ombrotrophic peatlands serve as an archive for atmospherically deposited cations and particulates. This is due to the fact that they receive water and inorganic nutrients solely from atmospheric deposition. *Sphagnum* cell walls also have a high cation-exchange capacity, which causes positively charged ions to respond strongly to the negatively charged functional groups on peat, immobilizing cations that are deposited via dry or wet deposition (e.g. Clymo et al. 1990, Merritt et al. 2004). Lead dating is based on the radioactive decay series of ^{238}U, a primordial nuclide that exists in all sediments, with a half-life of 4.46 x 10^9 years, which means that half of the original ^{238}U still remains (Merritt et al. 2004). In time, the ^{238}U in soil decays into ^{226}Ra, ^{222}Rn and eventually ^{210}Pb, which has a half-life of 22.3 years (Appleby & Oldfield 1978). By quantifying the ^{210}Pb inventory from the surface to a depth where ^{210}Pb is undetectable, it is possible to calculate the age-depth relations for a peat deposit. ^{210}Pb dating offers a reliable method to measure recent samples that cannot be reliably dated with carbon dating, allowing accurate radiometric dating of peat deposited over the past 150-200 years (Appleby & Oldfield 1978). Radiometric dating compares the number of remaining parent isotopes (^{238}U, ^{226}Ra, ^{222}Rn, ^{210}Pn) to the number of daughter products (^{210}Bi, ^{210}Po) present in the sample. ^{210}Pb activity can be measured directly from gamma emission or indirectly using either the beta

emitting daughter isotope ^{210}Bi or the alpha-emitting grand-daughter isotope ^{210}Po, which ^{210}Pb decays into eventually (Appleby & Oldfield 1978). For this thesis project, the samples were dated via *alpha spectrometry,* using ^{210}Po.

I personally carried out the lead dating procedure in June 2018 at the University of Exeter, United Kingdom. The dating was performed on every fourth sample, accounting into 64 samples in total. In my thesis only three peat sections were studied, so the number of dated samples relevant for this thesis is 48 samples. The procedure consisted of plating acid-digested peat samples with polonium-209 on silver discs. Firstly, the 48 samples of freeze-dried and grinded peat were weighed separately in acid washed beakers (the weight of the beaker was reduced). Then a 1 ml spike of ^{209}Po was added into the samples as a yield tracer. Next 10 ml of concentrated nitric acid (70% HNO$_3$) was added, and the samples were boiled on a hot plate until the HNO$_3$ had dissipated. The samples were removed from the hot plate and 10 ml of hydrogen peroxide (30% H$_2$O$_2$) was added to each sample. The samples were then heated and boiled again until dry. Afterwards, 5 ml of 6 molar hydrochloric acid (HCl) was added, boiled dry and repeated again. Next the samples were dissolved into 5 ml of 6M HCl for one hour. The samples were then poured into 40 ml centrifuge tubes and centrifuged 10 minutes at 2500 rpm. The supernatant liquid was then poured into acid washed plating jars that held a magnetic stirrer, and the jars were topped up with 40 ml of 0.5 molar HCl. A 0.2 g scoop of ascorbic acid was added to each sample. Then the painted and numbered lead disks were suspended into the liquid via fishing wire and the jars were closed and placed on a magnetic stirring table. The samples were allowed to stir for 24 hours. The following day the lead discs were rinsed with deionized water and brought to the counting room for alpha counting, which was performed by Matt Amesbury from the University of Exeter.

Once the results were ready, the data was processed into curves using the constant rate of supply (CRS) model, which assumes that the fallout of ^{210}Pb has been constant throughout time, and the supply decreases exponentially when moving from the surface to the bottom of the peat column due to radioactive decay over time (e.g. Appleby & Oldfield 1978, Le Roux & Marshall 2011). The results from the lead curves were then combined with the overlapping radiocarbon dates in R software via *Bacon* age-depth modelling, which uses Bayesian statistics to produce estimates of accumulation rates through combining radiocarbon and lead dates and information on accumulation rate (Blaauw &

Christen 2011). The default settings for the program were used. Bacon uses the IntCal13 calibration curve for radiocarbon dates (Reimer et al. 2013)

2.3.3. Peat and carbon accumulation

Bulk density measures the amount of mass in a given volume. For the bulk density analysis, at first labelled empty 5 cm^3 plastic containers were weighed, and the weights were marked into an Excel table. After weighing, the containers were filled with peat, using gentle pressure to remove air bubbles. The filled containers were covered with punctured Parafilm, frozen and cold dried. After the cold drying each container was weighed again and the weight difference between empty and filled containers was calculated. Bulk density was then calculated applying the following equation:

$$d = \frac{m}{V}$$

In which

d = bulk density of peat (g/cm^{-3})
m = dry mass (g)
V = fresh volume (cm^{-3}).

For this thesis, bulk densities were used to create the CRS model for the lead-dated samples, which requires bulk density, dry sample weight and ^{210}Pb concentration. Long-term accumulation of carbon was not measured because this thesis is focusing on hydrology and testate amoebae rather than carbon accumulation and peat composition.

2.3.4. Water table depth (WTD)

Historic reconstructions of water table depths are often used to show the past climate variability of a peatland. Water table depths can be reconstructed through transfer functions, which combine contemporary taxa to environmental variables and fossil data to create quantitative estimates (e.g. ter Braak & Juggins 1993, Woodland et al. 1998, Charman et al. 2007, Swindles et al. 2015c).

Reconstructions of past testate amoebae compositions were created in the C2 program via three commonly used models. Weighted averaging with tolerance downweighting and inverse deshrinking (WA-tol (inv)), weighted average partial least squares (WA-PLS) and the maximum likelihood model (ML) were run (e.g. Amesbury et al. 2013, Swindles et al. 2015b, Amesbury et al. 2016). According to the basic assumptions of these methods, different species occupy different niches in the environment. The occupied niches account to the tolerance ranges of the species. The weighted averaging methods work especially with multi-variable data with a large species composition (this allows also the absence of a taxon in several samples), a long ecological gradient, or a gradual change in abiotic factors in a long timescale. With each component, the models measure also the root mean square of the errors or RMSE (ter Braak & Juggins 1993).

The modern set used here is the pan-European testate amoeba training set by Amesbury et al. 2016, which suggests using the WA-tol (inv) model. Via the dataset the past water table depths could be reconstructed through transforming the proxy data of testate amoebae into deviations from the mean value, to depict trends instead of absolute values (see Väliranta et al. 2012). Then these transfer functions were applied to the fossil data. Samples were cross-validated using the leave-one-out (jack-knifing) technique (e.g Amesbury et al 2013).

3. Results

3.1. Chronologies

3.1.1. Radiocarbon chronologies

In total six samples were radiocarbon dated for this thesis, one from the bottom of the core (terminus of the active layer) and the other in the middle, with the following results:

Table 3. Radiocarbon chronologies. BP = age before present where 1950 AD is year zero.

Name and depth	Depth (cm)	^{14}C Age (BP)	Calibrated age (BP)
Taav 1.3 19	19	1064 ± 40 BP	990
Taav 1.3 40	40	2380 ± 30 BP	2415
Taav 2.2 13	13	70 ± 40 BP	80
Taav 2.2 49-50	49-50	7250 ± 40 BP	8080
Abi 2.2 21	21	156 ± 40 BP	120
Abi 2.2 39-40	39-40	835 ± 30 BP	740

The results indicate that the three studied peat cores are of markedly different age. The Taav 1.3 bottom age at 40 cm is 1705 years older than that of Abi 2.2 at the similar depth of 40 cm. Comparing Abi 2.2 with Taav 2.2 this age difference is as much as 7340 years, although the Taav 2.2 bottom age is taken 10 centimeters below the Abi 2.2 bottom age. A clear difference is visible also between the two Taavavuoma cores, despite them being located only 10 kilometers apart, with the Taav 2.2 bottom peat being 5665 years older than the Taav 1.3 bottom peat.

3.1.2. Lead chronologies

All three cores were supplementary dated with lead-210 with four centimeter accuracy. The background level of ^{210}Pb was reached at the Taav 1.3 core already at the depth of 15 cm, which was dated to 1834 AD. Since the radiocarbon date of 990 BP (960 AD) at 19 cm does not overlap with the lead data, the ages of the layers below 15 cm are uncertain.

For the other two cores the radiocarbon dates overlap the ^{210}Pb dates. For the Taav 2.2 core the depth 13 cm is ^{14}C dated to 80 BP (1870 AD). The ^{210}Pb date for the corresponding depth is 1933 AD. A similar effect is visible in the Abi 2.2 core, where the background ^{210}Pb activity level was reached not until 25 cm. The ^{14}C date at 21 cm is 120 BP (1830 AD), whereas the corresponding ^{210}Pb date is 1870 AD. Since the age gap between radiocarbon and lead dates in these two cores is small, they can be considered as reliable sources of information.
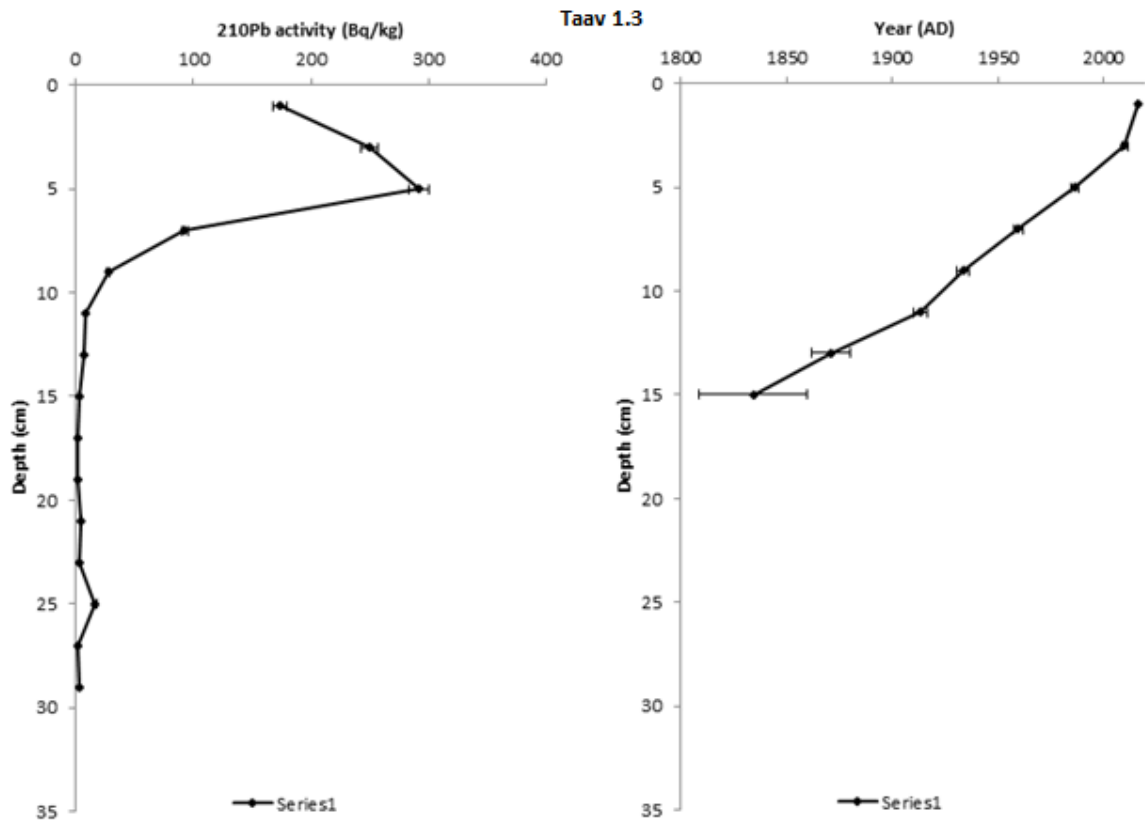
Figure 9. Lead dating results for the Taav 1.3 core. Left: ^{210}Pb activity (Becquerels / kilogram). Right: Age-depth model where ages are expressed as Anno Domini (AD) years. The activity decreases with age, which increases the uncertainty, shown as error bars.

Figure 10. Lead dating results for the Taav 2.2 and Abi 2.2 cores. Left: [210]Pb activity (Becquerels / kilogram). Right: Age-depth model where ages are expressed as Anno Domini (AD) years. The activity decreases with age, which increases the uncertainty, shown as error bars.
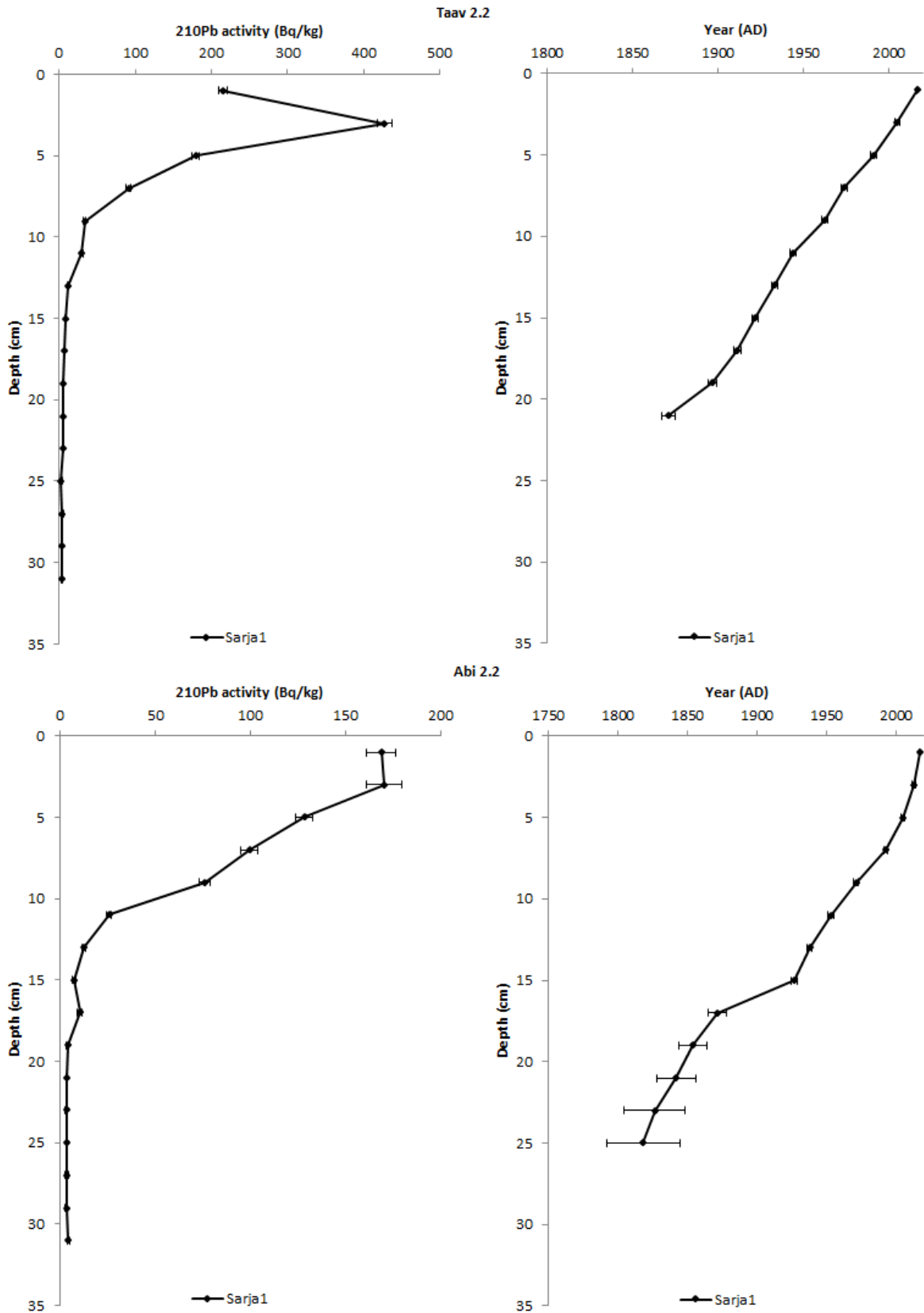
3.1.3. Age-depth models

The ^{210}Pb and ^{14}C dates were combined in R software to create Bayesian accumulation (Bacon) histories for deposits. The model produces an estimated minimum, maximum, median and weighted mean age for each centimeter of the core in years BP. The trustworthiness of these estimates decreases with age since fewer measurements exist due to the decay of ^{210}Pb, and thus the produced ages are based on extrapolation (Blaauw & Christen 2011). This is especially the case with the Taav 2.2. core, in which the ^{210}Pb measurements reach 21 centimeters or 1871 AD, and the remaining 29 centimeters encompasses a time span of over 7000 years, explaining the wide gray tail in Figure 12.

The Taav 1.3 output graph shows highest memory out of the three, whereas Abi 2.2 shows the lowest (Fig. 11 and 13), which indicates most stable environmental conditions for the Taav 1.3 core. In terms of accumulation rate, the Taav 2.2 (Fig. 12) core shows lowest overall accumulation. The Taav 1.3 core yields intermediate results with two peaks, whereas Abi 2.2 has had highest overall accumulation, but the most variability out of the three.

Since the testate amoebae were poorly preserved, thus not counted below 29 centimeters, the ages and depths below this can be considered irrelevant for the overall results. In other words, while the age graphs produce interesting output for discussion, as a whole they are relatively irrelevant for this thesis. For the analysed peat sections the testate amoebae assemblage data will be compared to the corresponding modelled age data to examine changes in hydrology.
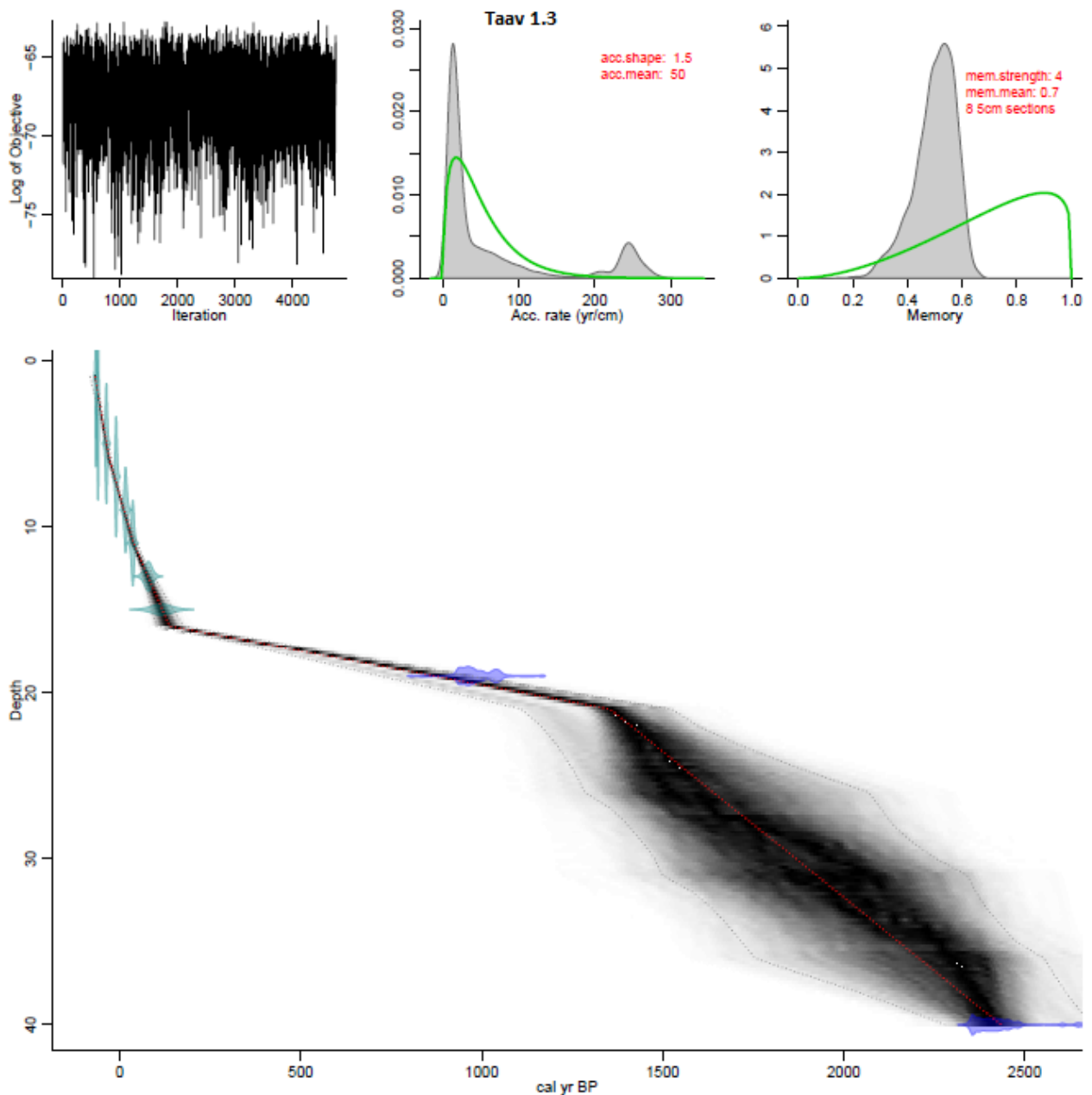
Figure 11. Bacon age-depth model for the Taav 1.3 core. Top left: number of Markov Chain Monte Carlo (MCMC) iterations, estimating the accumulation rate in years/cm. Good runs show little structure among neighbouring iterations. Top middle: information on accumulation rate. Top right: memory or variability of accumulation rate. High memory implies constant accumulation history, whereas low memory indicates variable environmental conditions over time. Bottom: calibrated ^{14}C dates (dark blue) and calibrated ^{210}Pb dates (light blue), and the age depth model. Darkness of curve indicates likeliness of estimated age, grey dotted line shows 95% confidence intervals, and red curve shows single best model based on the weighted mean age for each depth (Blaauw & Christen 2011).

Figure 12. Bacon age-depth model for the Taav 2.2 core. Top left: number of Markov Chain Monte Carlo (MCMC) iterations, estimating the accumulation rate in years/cm. Good runs show little structure among neighbouring iterations. Top middle: information on accumulation rate. Top right: memory or variability of accumulation rate. High memory implies constant accumulation history, whereas low memory indicates variable environmental conditions over time. Bottom: calibrated 14C dates (dark blue) and calibrated 210Pb dates (light blue), and the age depth model. Darkness of curve indicates likeliness of estimated age, grey dotted line shows 95% confidence intervals, and red curve shows single best model based on the weighted mean age for each depth (Blaauw & Christen 2011).
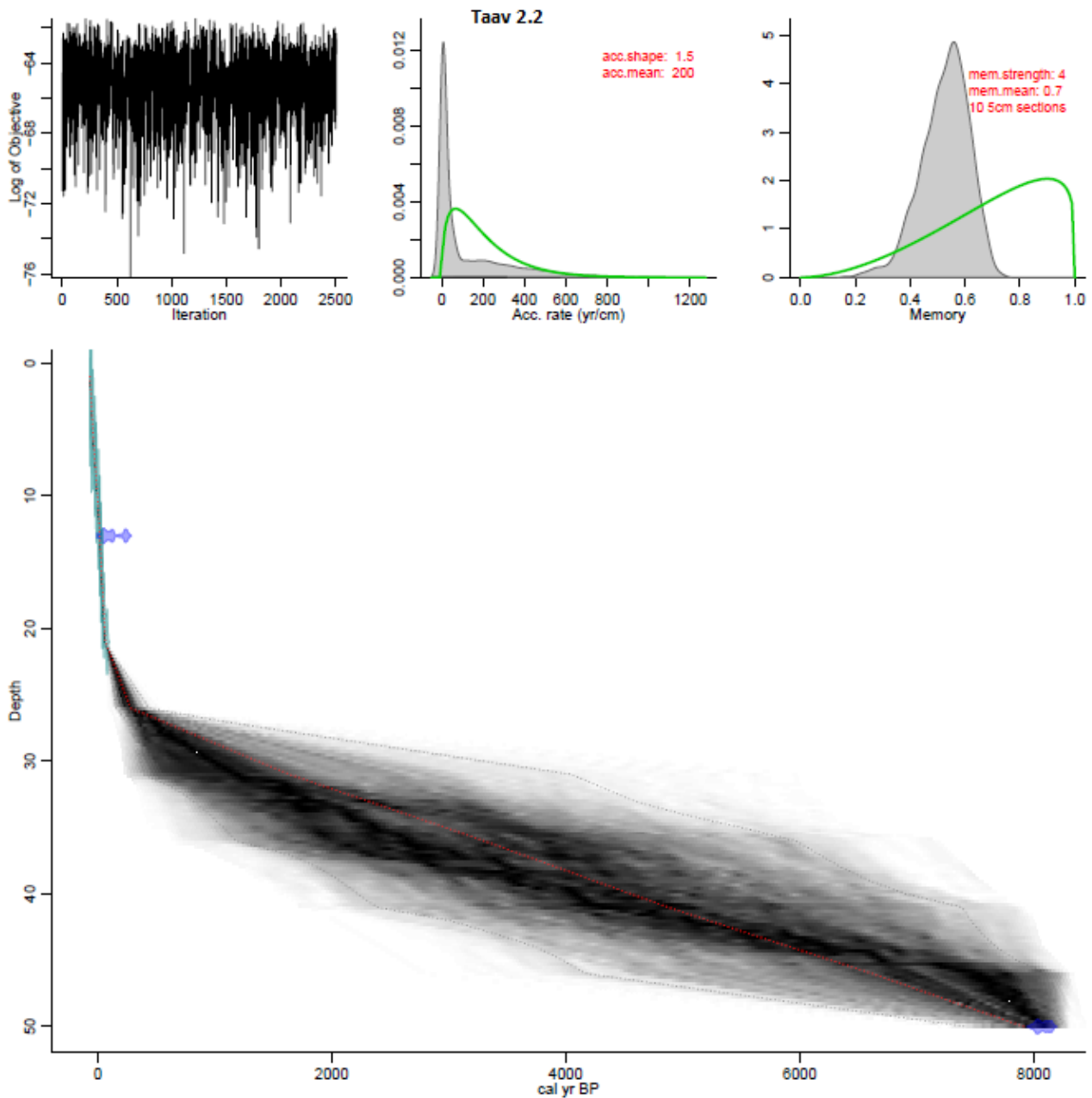
Figure 13. Bacon age-depth model for the Abi 2.2 core. Top left: number of Markov Chain Monte Carlo (MCMC) iterations, estimating the accumulation rate in years/cm. Good runs show little structure among neighbouring iterations. Top middle: information on accumulation rate. Top right: memory or variability of accumulation rate. High memory implies constant accumulation history, whereas low memory indicates variable environmental conditions over time. Bottom: calibrated 14C dates (dark blue) and calibrated 210Pb dates (light blue), and the age depth model. Darkness of curve indicates likeliness of estimated age, grey dotted line shows 95% confidence intervals, and red curve shows single best model based on the weighted mean age for each depth (Blaauw & Christen 2011).
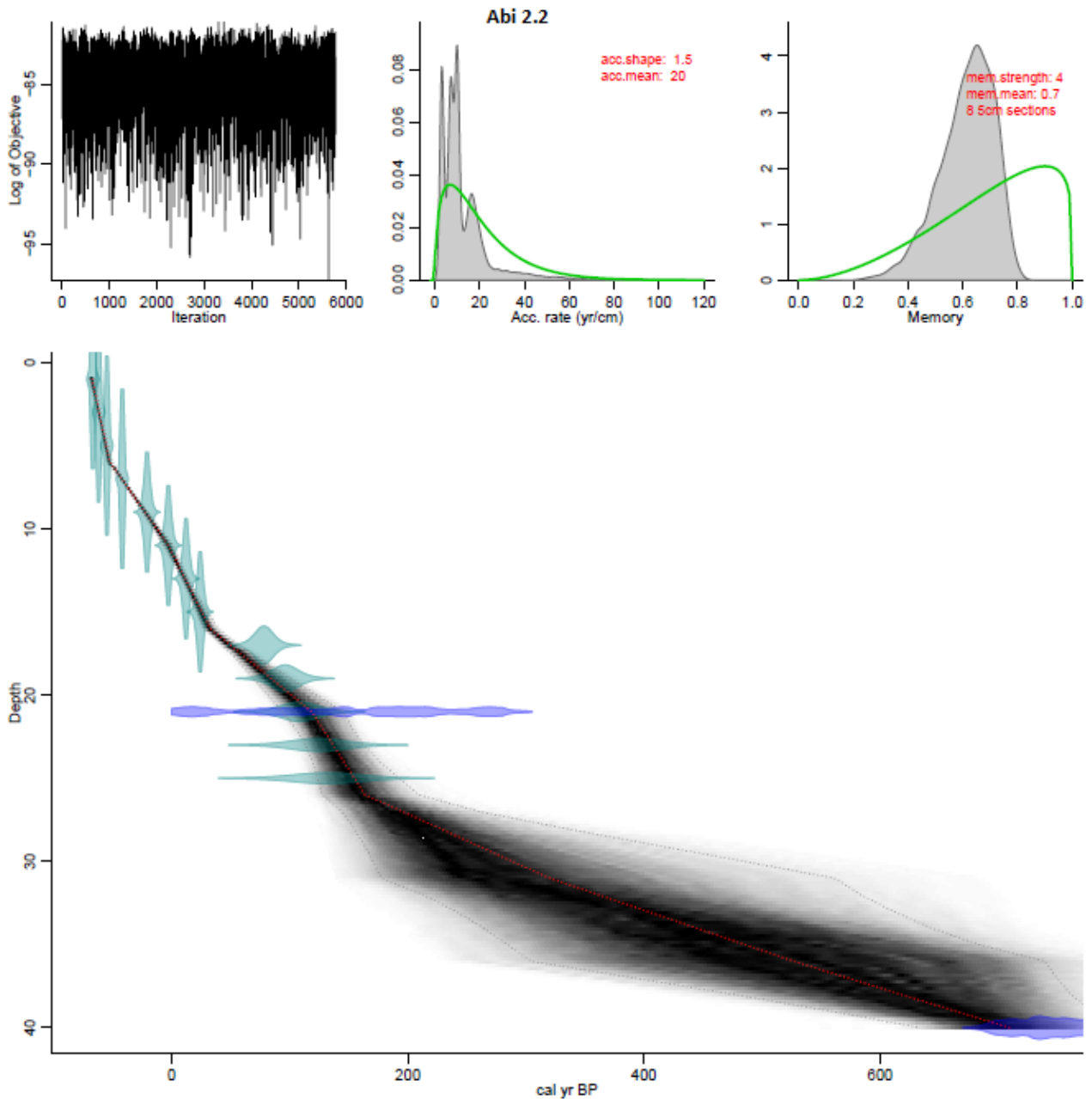
3.2. Testate amoebae data

A total of 39 different taxa were identified from the samples. Site-specifically there were 35 taxa from Abi 2.2, 29 taxa from Taav 2.2 and 27 from Taav 1.3. Most abundant 15 taxa are presented in Figure 14. Figures 16-18 depict the species assemblages per core, listed next to date (AD) and reconstructed water table depth. The species are assorted in descending order from wet to dry according to the classification used by Zhang et al. (2017). Species with a less than 5 % occurrence in a single core are not presented in the diagrams.
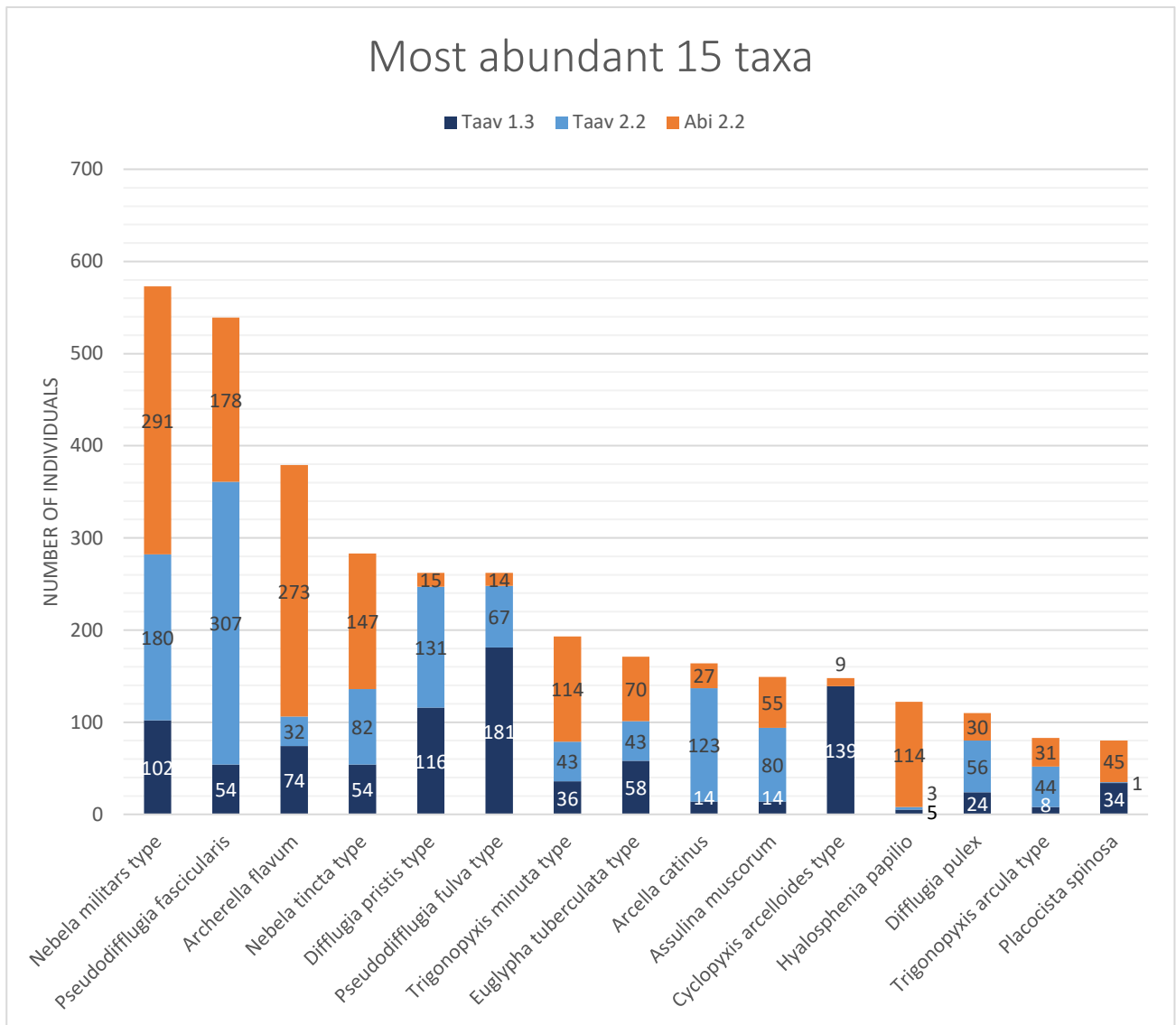

Figure 14. Most abundant 15 taxa. Taavavuoma taxa marked with blue, Abisko taxa with orange.

3.2.1. Taav 1.3

Taav 1.3 was the least diverse in terms of identified taxa. The overall number of counted specimens was also the lowest. A count of 100 specimens within a reasonable time frame was possible only until the depth of 15 centimeters. Below this precise identification became increasingly more difficult due to the high abundance of obscuring plant debris, which made important features such as aperture shape and test texture indistinguishable. A new preparation round was run on the sub-sample, using a 180 µm sieve instead of 300 µm, but the problem persisted. 50 specimens were counted until 23 cm, after which it became nearly impossible due to high level of decomposition. This depth coincides with the same depth where the ^{210}Pb reaches its lowest activity (Fig 9.) At this depth the composition of the peat also changes from light *Sphagnum* peat to well-humified, dark *Carex*-peat (Figure 5).

The five most abundant taxa were *Pseudodifflugia fascicularis* (181), *Cyclopyxis arcelloides* type (139), *Difflugia pristis* type (116), *Nebela militaris* type (102) and *Archerella flavum* (74). In contrast to the other cores, *Cyclopyxis arcelloides* and *Pseudodifflugia fulva* stood out with their abundance, the former being completely absent in the other Taavavuoma core, and the latter being two times less abundant in the other Taavavuoma core and close to absent in Abisko.

Starting from the bottom of the core at 451 AD, the deep layers proved the most difficult to interpret due to high abundance of plant debris and the considerable time gaps of ca. 500 years between 17-21cm. *Difflugia lucida, Placocista spinosa, Trigonopyxis arcula* and *Trigonopyxis minuta* were abundant from 481 AD to 1083 AD. At 1570 AD a change occurred, and *Cyclopyxis arcelloides* dominated the segment with over 60% abundance, although it was completely absent in the deeper layers. After this the time gap between segments shortens considerably.

The dominant species from 1833-1912 AD were *Pseudodifflugia fulva* and *Cyclopyxis arcelloides,* although the abundance has decreased to 20%. The abundant presence of *P. fulva* was taken over by *Pseudodifflugia fascicularis* around 1936 AD.

Nebela tincta and Nebela militars showed an increase from 1936 AD onwards, whereas *Difflugia pristis and Pseudodifflugia fulva* decreased approaching the upper layers. *Trigonopyxis minuta* and *Trigonopyxis arcula* peaked at 1986 AD, although their abundance remained below 20%. The

uppermost 3 cm peat layers from the 21st century onwards were almost entirely characterized by an increasing amount of *Nebela tincta* and *Nebela militars* types and *Archerella flavum.*
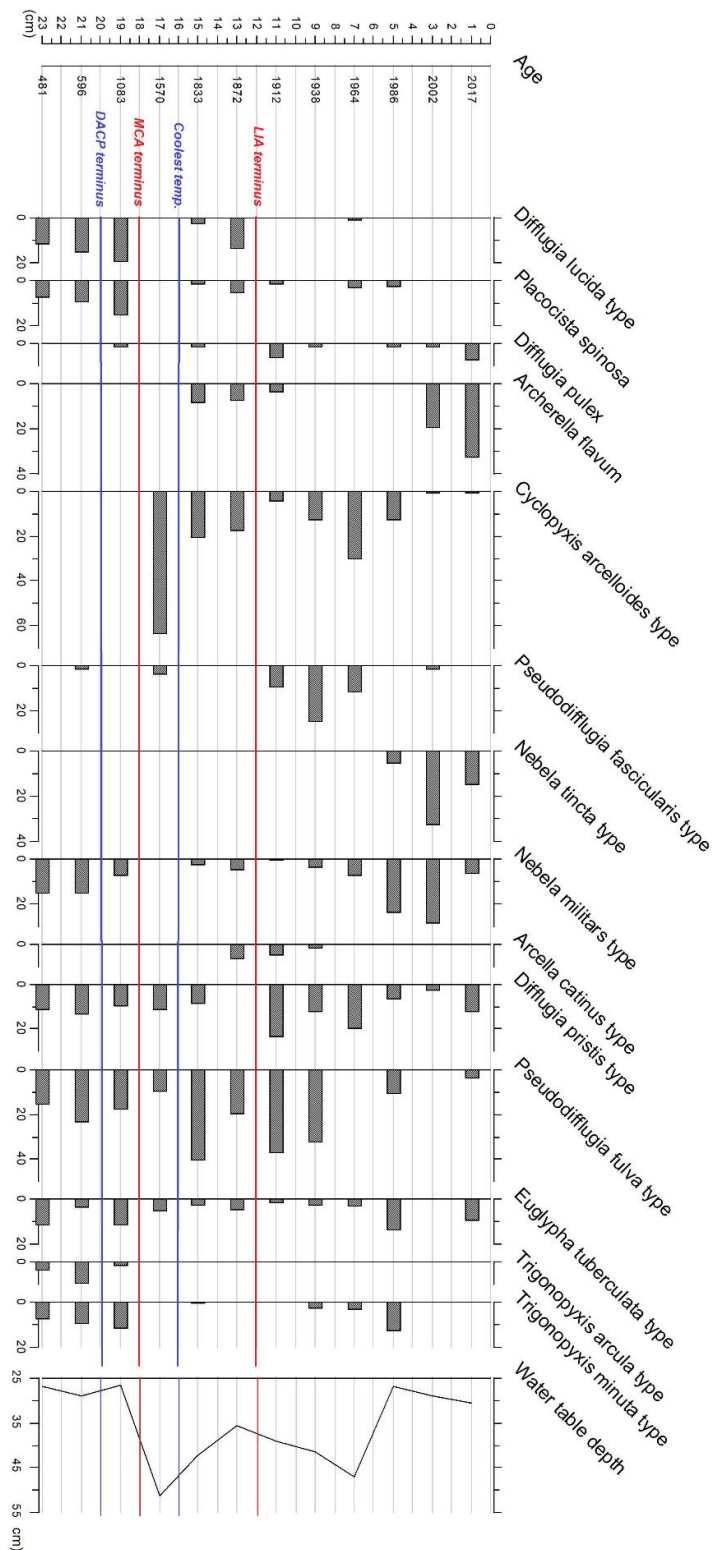

Figure 15. Taav 1.3 core age (AD), counted specimens (percentages), and water table depth (WAPLS). Colored horizontal lines indicate cold and warm periods as told in Ch 1.2. Coolest temp = coldest LIA temperature at 1750 AD (Treat & Jones 2018).

38

3.2.2. Taav 2.2.

Taav 2.2 fell in between the two other cores in terms of diversity. A count of 100 specimens was possible until the depth of 21 centimeters, after which 50 specimens were counted until the depth of 29 centimeters. The most abundant five taxa were *Pseudodifflugia fascicularis* type (307), *Nebela militars* type (180), *Difflugia pristis type* (131), *Arcella catinus type* (123), and *Nebela tincta type* (82).

The bottom of the core was dated to 851 AD. At first *Arcella catinus* acted as the dominant species with over 60% abundance. After this the taxa became considerably less abundant and never reached 20% abundance. During 1394 AD, *Pseudodifflugia fascicularis* became the dominant taxa with 60% abundance. Abundance remained at 40% until 1799 AD, when it momentarily fell to 20%, and rose back to 40% at 1885 AD. The year 1799 AD was also a peak year for *Difflugia pulex,* which acted as the dominant taxa with 30% abundance. *Difflugia lucida* also became absent after this year. At the same time a slight increase happened in *Difflugia pristis* until 1897 AD.

At 1910 AD *Nebela tincta* reappeared, being last time observed at 1799 AD. At the same time *Nebela militars* started growing in abundance. Both taxa increased in abundance as the 20th century progressed, and the modern sample was clearly dominated by *Nebela tincta* with 40% abundance.

Strictly dry taxa such as *Trigonopyxis arcula, Trigonopyxis minuta* and *Assulina muscorum* seem to have played a small role in the past of this core, with only small abundances throughout the core, and a 20% peak abundance in *T. arcula* at 1977 AD and *Assulina muscorum* at 2004 AD.
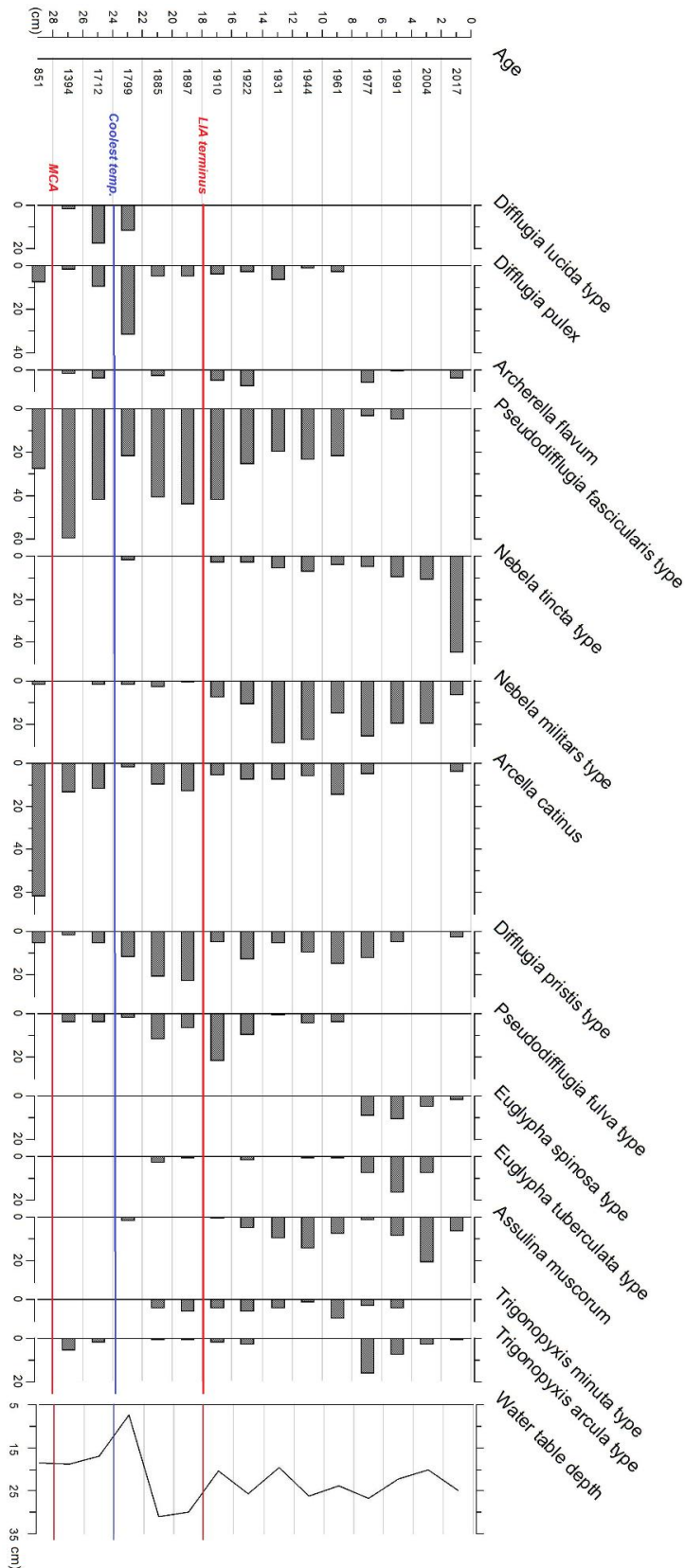
Figure 16. Taav 2.2 core age (AD), counted specimens (percentages), and water table depth (WAPLS). Colored horizontal lines indicate cold and warm periods as told in Ch 1.2. Coolest temp = coldest LIA temperature at 1750 AD (Treat & Jones 2018).

40

3.2.3. Abi 2.2.

Abi 2.2 had the highest diversity and specimen count out of the three cores. The count of 100 specimens was possible until the depth of 29 centimeters, and in many cases the samples were abundant enough to easily allow the count of over 100 specimens, especially in the 8-9 cm segment, in which a 1 ml sample contained 138 counted specimens within a single glass plate. Since the ages of the entire column are fairly recent and large time gaps do not occur, the results of this core can be considered having the best resolution.

The most abundant five taxa were *Nebela militars* type (291), *Archerella flavum* (273), *Pseudodifflugia fascicularis* type (178), *Nebela tincta* type (147), and *Trigonopyxis arcula* and *Hyalosphenia papilio* types, both with 114 specimens. Already this separates the Abi 2.2 cores from the Taavavuoma cores, in which *A. flavum* and *H. papilio* were significantly less abundant.

History of the core began 1693 AD. During this time dominant taxa were *Trigonopyxis minuta* and *Pseudodifflugia fascicularis* with ~25% abundance. Both decreased in abundance as time progressed, and *T. minuta* became completely absent after 1813 AD. *Trigonopyxis arcula* appeared in small amounts until 1866 AD and made a single appearance at 1939 AD.

After 1813 AD, *Nebela tincta* and *Archerella flavum* seem to have played a larger role, the former of which was absent before this time. *A. flavum* peaked in 40% abundance from 1900-1925 AD, after which only few specimens were present. *Nebela militars* was present in all samples, but peaked at 40% abundance 1939 AD, after the fall of *A. flavum.* The peak of *N. tincta* lagged slightly behind, ranging from 30-25% during 1973-1993 AD. After this *A. flavum* made a comeback and increased from 15 to 40% in abundance between 2005-2017 AD. Another notable taxon is *Hyalosphenia papilio,* which appeared originally at 1813 AD. The taxon was temporarily absent 1866 and 1939 AD, but appears abundant in recent layers, rising from 5 to 20% in abundance from 1953 AD onwards (with the exception of a slight decrease at 2005 AD).
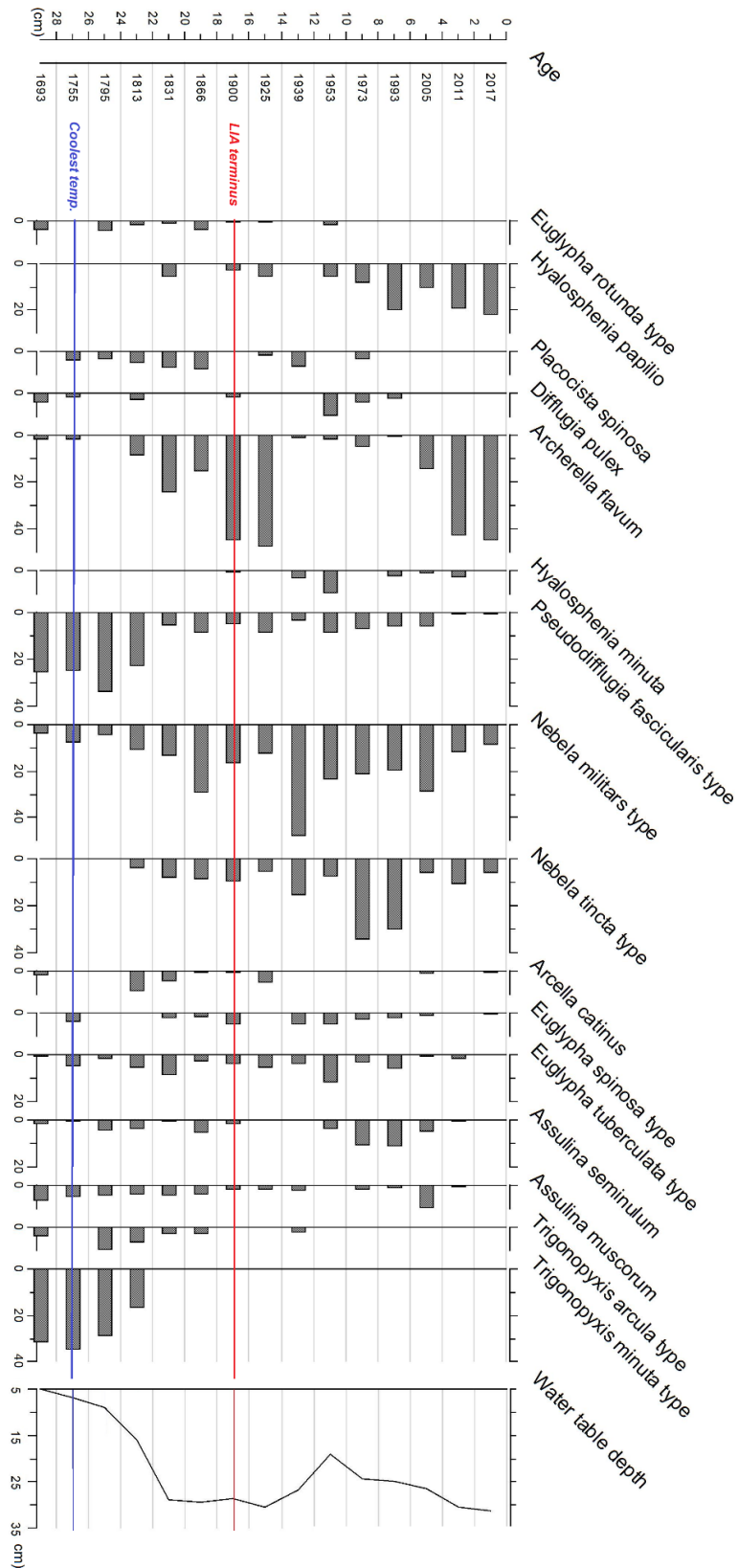
Figure 17. Abi 2.2 core age (AD), counted specimens (percentages), and water table depth (WAPLS). Colored horizontal lines indicate cold and warm periods as told in Ch 1.2. Coolest temp = coldest LIA temperature at 1750 AD (Treat & Jones 2018).

42

3.3. Water table depth reconstructions

Out of the three model runs (weighted averaging with tolerance downweighting and inverse deshrinking (WA-tol (inv)), weighted average partial least squares (WA-PLS) and the maximum likelihood model (ML)), the model with the lowest root mean square error of prediction (RMSEP) and highest coefficient of determination (r2) was chosen.

The results for the water table reconstructions confirmed the suitability of the WA-tol (inv) model. WA-tol (inv) performed best, providing an RMSEP 7.07562 and an r2 value of 0.612149. This implies that ~61% of the variability has been accounted for, making the model fairly reliable. Previous studies such as Amesbury et al. (2013), Amesbury et al. (2016) and Swindles et al. (2015b) have yielded similar results, proving that the WA-tol (inv) model is recommendable in water table reconstructions due to low RMSEP and high r2 values.

The regression model graphs were later added into the testate amoebae result graphs (Fig. 15-17).

Table 4. Model performance statistics. For the WAPLS model the C2 stands for second component. Jack stands for jack-knifing (leave-one-out cross validation).

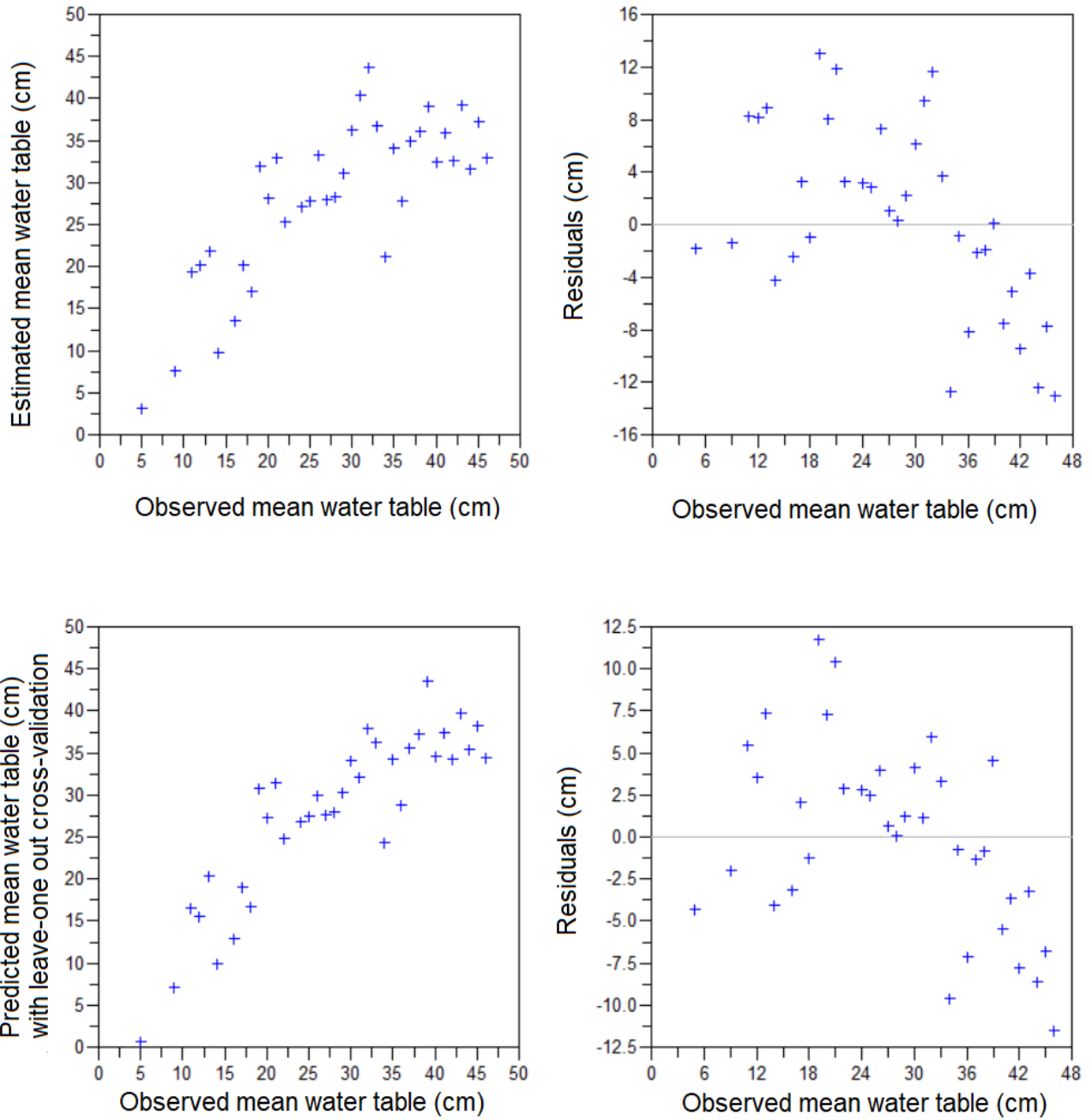| **Model**	**RMSEP (jack)**	**R2 (jack)**
WA-tol (inv)	7.07562	0.612149
WAPLS-C2	7.47386	0.593811
ML	7.53581	0.602298

Figure 18. (a, b) WA-tol regression model transfer function which acts as a base for the water table reconstruction. (c) relationship between predicted mean water-table and the modern water table depth. (d) model residuals.

4. Discussion

4.1. Climatic fluctuations over the Holocene period

The Holocene has overgone various notable climatic phases, all of which have presumably affected peatlands differently:

1) The Holocene Thermal Maximum 11000-5000 BP
2) Roman Warm Period 1-300 AD
3) Dark Age Cold Period 300-800 AD
4) Medieval Climate Anomaly 800-1300 AD
5) Little Ice Age 1300-1900 AD
6) Post-industrial temperature increase 1900 AD -> (e.g. Broecker 2001, Ljunqvist 2010).

Out of these periods, the HTM, the RWP, the MCA and the post-industrial temperature increase have been identified as warmer periods (Cook et al. 2015), whereas the DACP and LIA have been classified as cold periods (Wanner et al. 2011). Previous studies have identified cold periods such as the LIA as periods of slow peat accumulation due to lowered primary production and surface freezing processes (Mauquoy et al. 2004, Zhang et al. 2017 & 2018). Similarly, many models have linked colder periods to higher water tables and wetter conditions (e.g. Swindles et al. 2015c).

My research hypotheses were the following:

1. *In peat records cold and warm periods can be observed via changes in moisture conditions, with warm periods commonly corresponding with dry and cold periods with wet conditions.*
2. *"The present is the key to understand the past" - Arctic peat layers contain moisture sensitive testate amoebae which allow the reconstruction of past climatic events.*

My research questions were:

1. *What kind of changes the testate amoebae compositions have experienced in the past?*
2. *Are the newly-reconstructed changes in hydrology comparable to previous climate reconstructions?*

The first research hypothesis is proven true, since the peat cores contain information in the form of testate amoebae assemblages and peat composition changes. The second hypothesis is more difficult to prove. The fact that species assemblages in different cores were not temporarily coherent suggests an underlying driving factor, such as abiotic conditions, hydrology or temperature, or biotic factors such as vegetation and competition with other species. Assumed that climatic events are reflected in

changes in moisture conditions and thus species assemblages, a similar response should be regionally visible. It is also possible that in some cases the reconstructions fail to represent reliable climatic conditions that prevailed at a certain point of time due to limited ecological knowledge of taxa, false identification (Payne et al. 2011, Tolonen et al. 1992), or non-climate related events, such as fires (Tuittila et al. 2017) that have affected the species composition.

4.2. Late Holocene climate periods and Arctic peatland hydrology

The cores studied in this thesis were of different ages. The Abisko core was the youngest, allowing the inspection of events from 1693 AD onwards. Although the Taav 2.2 core is older than the Taav 1.3 core, the testate amoebae data in the aforementioned core reached only until 851 AD, whereas the deepest deposits in the Taav 1.3 core were dated to 481 AD. Thus, in this thesis, roughly the past 320 years can be explored with the highest resolution, including the mid-to late Little Ice Age and post-industrial temperature increase. Both Taavavuoma cores also allow the exploration of the Medieval Climate Anomaly. Only the Taav 1.3 core gives insight on older climatic periods. The following chapters will focus on the climate history of the past millenium, beginning with the Dark Age Cold Period, with the aim of identifying the discrepancies and similarities between the testate amoebae-driven water table reconstructions and previous climate reconstructions.

4.2.1. Dark Age Cold Period

The Dark Age Cold Period (sometimes referred to as Dark Ages Cold Period), DACP, was a climatic phase occurring roughly from 300-800 AD (e.g. Broecker 2001, Ljunqvist 2010). In this thesis the bottom segments of the Taav 1.3 core represent the DACP. The most common species from 481-596 AD were intermediate and dry taxa such as *Pseudodifflugia fulva* type*, Nebela militaris* type and *Trigonopyxis* spp. (Zhang et al. 2017). The result of the water table reconstruction indicates that this was an intermediate-dry period, with water table depths around 25 cm. However, when comparing this WTD value to the values reconstructed for the other climate periods from the same core, the DACP actually seems to be wetter than usual, and thus appears as a wet "peak" in the reconstruction. This is due to the appearance of the wet taxa *Difflugia lucida* type and *Placocista spinosa.* This is an interesting result considering the ecology of these two, of which the former has a narrow water table range indicating even hollow conditions. However, simultaneous presence of both dry and wet taxa

is not necessarily contradictory. Previous studies such as Charman et al. 2007 and Zhang et al. 2017 have found that dry taxa have larger tolerance ranges than wet taxa, and often can occur in small quantities in wet locations. Yet whether it is possible for such a strictly wet taxon like *Difflugia lucida* to appear in dry conditions is a matter addressed further in Chapter 4.3 and could possibly be the result of identification error caused by the mixup with the dry-intermediate, but similar-looking *Difflugia pristis.*

The coexistence of both wet and dry taxa may possibly be an indicator of variable conditions at the coring site (Zhang et al. 2017). This could be a result of the DACP being a period of unstable climate as suggested by Helama et al. 2017. Short-term hydrological fluctuations are seen as simultaneous presence of wet and dry testate amoebae taxa. This result supports the variable DACP hypothesis, but since it is only one data set, further measurements would need to be taken to make conclusions of a larger phenomena. It is notable that each sample in this thesis represents roughly a period of one year and the conditions of a coring site may change also seasonally, potentially affecting the composition.

4.2.2. Medieval Climate Anomaly

The Medieval Climate Anomaly and the Little Ice Age are possibly the most widely studied periods of the late Holocene, and several studies have identified significant shifts in water tables during these periods (e.g Väliranta et al. 2007, Swindles et al. 2015a and Zhang et al. 2017 and 2018). The MCA occurred roughly from 800-1300 AD (e.g. Broecker 2001, Ljunqvist 2010). In this thesis the MCA covers the 19 cm segment, bottom age 1083 AD in the Taav 1.3 core, and for the Taav 2.2 core age of the bottom segment is 851 AD.

In Taav 1.3, no changes in species composition happened between 19 cm and 21 cm, despite the measurements being from two different climatic periods and roughly 500 years apart. Thus, the water table reconstruction paints a similar picture of the MCA as with the DACP, indicating this to be a period of variable climatic conditions with both wet and dry taxa being apparent. The water tables during this period are on average around 25 cm. The Taav 2.2 core water table reconstruction suggests that the WTD is roughly 17 cm, as dominated by the intermediate taxa *Pseudodifflugia fascicularis* and *Arcella catinus.* Much like in the Taav 1.3 core some wetter taxa are also present, in this case

Difflugia pulex. However, this is a taxon with a wide water table tolerance and the ability to survive in relatively low moisture content (Charman et al. 2007, Zhang et al. 2017).

When comparing the two cores, the Taav 2.2 core supports the hypothesis of the MCA as a drier period before the wetter LIA. A study by Linderholm et al. 2018 compiled together multiple proxy data from Fennoscandia, such as tree ring data, estimates of peat humidification and varve thickness, and also found that a majority of the records supported wetter conditions only when approaching the LIA. Cook et al. (2015) and Väliranta et al. (2007) also claim the MCA being a drier period. In contrast, the Taav 1.3 core appears to have experienced wetter conditions during the DACP and the MCA rather than during the LIA, although the conditions were never as wet as in the other study sites. Some studies such as Väliranta et al. 2007 and Langdon & Barber 2005 have identified a wet period roughly from 750-1250 AD, which coincides with the end of the MCA and the data of the Taav 1.3 core. Thus, much like the DACP the MCA could be called a period of a disputed climate caused by local variation.

4.2.3. Little Ice Age

The Taav 2.2 core contains information on the LIA ranging from roughly 1394 AD to 1897 AD. The Taav 1.3 core gives us further insight to the period between 1570-1872 AD. Lastly, Abi 2.2 contains high resolution information on the late LIA period, ranging from or 1693-1900 AD.

Beginning from the Taav 2.2 core, the water table reconstruction shows that the LIA began as a relatively dry period with water tables close to 20 cm, after which conditions became gradually wetter until they reached a peak of 7 cm depth at 1799 AD. This coincides well with the observations of Treat & Jones (2018) that the coldest LIA temperatures occurred around 1750 AD. Moreover, the mid-LIA wet periods have been recorded by several studies for the Scandinavian region and for the British Isles (e.g. Hughes et al. 2000, Langdon & Barber 2005, Väliranta et al. 2007). After this the records indicate a sharp drop in WTD to 30 cm during 1855 AD, and the rest of the LIA was clearly a dry period, although there was a slight trend towards wetter conditions towards the LIA terminus.

A deeper analysis on the taxa driving the reconstruction shows that the taxa benefiting of the the early LIA conditions were the wide-range intermediate *Pseudodifflugia fascicularis* and wet *Difflugia* taxa,

especially *Difflugia pulex*. It is considered as ecologically poorly know taxon which is, for some reason, often common in fossil assemblages but rare in surface training set samples. It has an almost identical water table optimum to the usually abundantly present wet-intermediate identicator *Archerella flavum* (Amesbury et al. 2013). Interestingly however the latter was completely absent during the 1799 AD segment despite the similar optima. The studies by Sullivan & Booth (2011) and Zhang et al. (2017) note *A. flavum* seems to be more abundant in relatively stable hydrological conditions, when *D. pulex* can also survive short-term hydrological fluctuations. Considering that the proportion of *D. pulex* prominently decreased after the 1799 AD segment it is possible that at Taav 2.2 site the beginning of the LIA was a period of rapid change towards wetter conditions which roughly lasted for three centuries. *D. pulex* and *P. fascicularis* may have benefited from this change due to their wide water table optimas and high adaptability (Zhang et al. 2017). After this the sharp drying recorded at 1886 AD coincides with the decrease of the proportion of *P. fascicularis*, which was replaced by the *Difflugia pristis,* which is largely driving the construction during that time. The species composition remained relatively unchanged until the end of the LIA.

Out of the three cores the Taav 1.3 core shows the most pronounced change between the MCA and the LIA. The reconstruction shows that during this period the water tables fell from 25 cm at 1570 AD to as low as 50 cm. This is extremely low even for dry taxa. Both the exclusively wet and dry taxa disappeared, and the segment was almost completely dominated by the wide-range wet-intermediate indicator *Cyclopyxis arcelloides* type. As the LIA proceeded some wet taxa returned and the water tables gradually rose to their peak of ~35 cm during 1872 AD. The large amount of *C. arcelloides* makes the data difficult to interpret: Amesbury et al. (2013) noted that the large abundance of a single taxon is a common source of reconstruction anomalies. However, this period clearly deviates from the long-term mean water tables and thus could be a strong signal for a climatic fluctuation instead of changes in internal dynamics (e.g. Gunnarsson et al. 2002). *C. arcelloides* is a taxon with a wide water table optimum (Zhang et al. 2017) and thus most likely benefited of the changing circumstances on the expense of other taxa.

Finally, the Abi 2.2 core gives an insight on the late LIA from 1693 AD onwards. According to the reconstructions the coring site experienced extremely wet conditions at first, with the water tables at 5 cm from the surface. As the LIA progressed conditions became drier and drier, until water tables reached a depth of roughly 30 cm at 1831 AD and stayed similar until the LIA terminus. The species

composition during this time consisted mainly of wet-intermediate *Pseudodifflugia fascicularis* and the dry *Trigonopyxis minuta* type. In this case it is notable that the aforementioned taxon appears to overrule the influence of the latter (WTD optimum for *P. fascicularis* is 11 cm) and draws the water table to a higher depth than what would be the optimum for *T. minuta* (27 cm). As indicated before with the case of both Taavavuoma cores, it is feasible for dry taxa to occur in wet locations due to their wide tolerance ranges (Charman et al. 2007). It is also possible that the non-realistic water table reconstruction is caused by an anomaly due to the high dominance of two taxa with seemingly different optimas (Amesbury et al. 2013). Based on the reconstruction however it seems that the Abi 2.2 site experienced a similar trend as the Taav 2.2 coring site, with the ecosystem being at its wettest during the 18th century, which coincides with past studies identifying a major rise in water table depths during the time (e.g Väliranta et al. 2007, Swindles et al. 2015a and Zhang et al. 2017 and 2018). The Taav 1.3 core stands out with its opposite moisture trend when compared with the two other cores.

4.2.4. *Post-industrial warming*

Lastly, the post-industrial warming, beginning from roughly 1900 AD, can be observed from all three cores. Out of the cores, in Taav 1.3 only six samples were from this time period. In this core no major changes happened in species composition between the LIA and the post-industrial warming. The water table depth reconstructions indicate that the water table was between 35-40 cm during the terminus of the LIA, and began to fall until 1964 AD, when it was between 45-50 cm. During this time there was a lack of wet taxa and a peak in *Cyclopyxis arcelloides* and *Difflugia pristis,* which seem to be the species driving the reconstruction. Around 1986 AD the WTD was highest, i.e. 25 cm. After this WTD has remained roughly the same, although with a slight drying trend. During modern times there has been a clear shift in species composition with intermediate *Nebela* taxa and wet-intermediate *Archerella flavum* replacing *C. arcelloides* and *Pseudodifflugia fulva* as dominant taxa.

The Taav 2.2 core shows that the end of the LIA appears to have been drier than the beginning of the post-industrial warming period. There were two slightly wetter peaks at 1910 AD and 1931 AD, and two slightly drier drops at 1922 AD and 1944 AD, respectively. Approaching modern times, the reconstruction curve shows a smoothening trend towards wetter conditions, until there is a slight drop at 2017 AD. Overall throughout the past century the water table depths have remained relatively

unchanging and within 20-25 cm range. The species composition shows a rather clear shift from the dominance of *Pseudodifflugia fascicularis* to an increase in *Nebela* taxa.

Much like in the other two cores, no major changes happened in the Abi 2.2 core at the LIA terminus considering the species composition. The water table reconstructions show that the post-industrial warming period began as dry, with water tables at ~27 cm. During 1939-1953 AD the coring site became wetter and water tables rose 10 cm. This coincides with some previous studies that identified an Arctic warming period from 1920 to 1940, followed by a minor cooling from 1940-1970, after which the climate began to warm again (e.g. Overland et al. 2004, Serreze & Francis 2006). The species driving this reconstruction are largely intermediate *Nebela* taxa and the wet and wet-intermediate *Hyalosphenia papilio* and *A. flavum.* The wet peak during 1953 AD appears to be largely explained by the rise of *Difflugia pulex.* Based on species data only, it seems that wet-favoring taxa have become more abundant when approaching the modern times. This anomaly could be explained by the high dominance of *A. flavum* adversely affecting the reconstruction as indicated by Amesbury et al. 2013, the lack of driving wet taxa such as *D. pulex* and *P. fascicularis,* or that the ecological traits of the taxa at the coring site differ from that of the training set taxa (Zhang et al. 2017).

In brief both the Taav 2.2 and Abi 2.2 site have become drier during the post-industrial warming period, with the exception of a few short term wet peaks, which in the Abisko site could be explained by a possible cooling period during the mid 20th century (e.g. Overland et al. 2004, Serreze & Francis 2006). The Taav 1.3 site is an exception, having experienced a major wet shift in the mid-20th century, after which the site has not returned to its previous state. Compared to the contemporary water table depth measurements at the sites (20 cm at Taav 1.3, 22 cm at Taav 2.2 and 13 cm at Abi 2.2), the reconstructions appears to exaggerate the dryness for all three sites (30 cm for Taav 1.3, 25 cm for Taav 2.2 and 30 cm for Abi 2.2). Based on the contemporary water table measurement only, the reconstruction for Taav 2.2 is the closest to the reality.

4.2.5. *Comparisons between sites*

A comparison between the study sites of this thesis reveals three different climatic reconstructions for four climatic periods of the Holocene: the Dark Age Cold Period, the Medieval Climate Anomaly, the Little Ice Age and the post-industrial warming. Only the Taavavuoma cores covered the DACP

and MCA, and a mixed species composition points towards unstable climatic conditions during these times (Helama et al. 2017, Zhang et al. 2017). Approaching the LIA, the difference between these two study plots becomes visible, as the Taav 1.3 site shows a drying trend approaching the LIA, when the trend at Taav 2.2 is the opposite, i.e. wetting. The data from the latter site coincides very well with climatic data indicating cold and wet conditions during the LIA (e.g. Treat & Jones 2018, Swindles et al. 2015a, Väliranta et al. 2007). The water table reconstruction from Abisko also points towards the LIA as a wet period. After the terminus of the LIA both the Abi 2.2 and Taav 2.2 sites have showed little variation, but the overall trend points towards drying conditions during the past century. Since water table depth is positively correlated with temperature, the drying could be explained by an increase in evapotransporation caused by a warming climate (Swindles et al. 2015a). The Taav 1.3 site once again indicates the opposite.
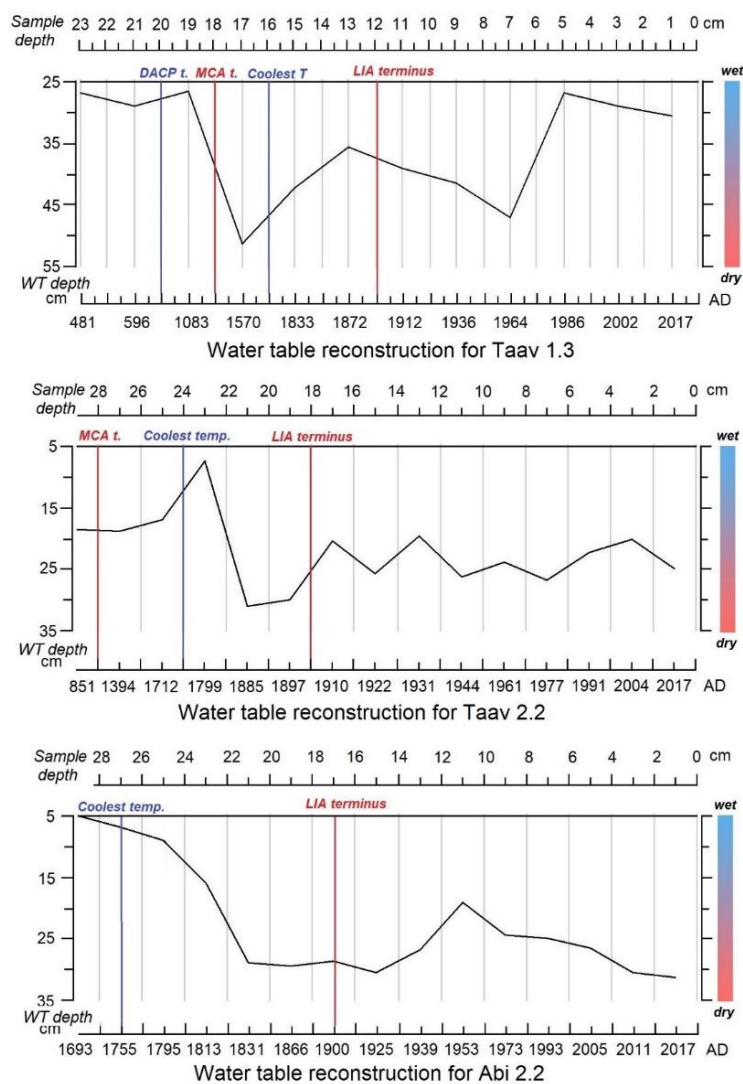

Figure 19. Water table reconstructions for the three study sites. Compared to climatic periods.

Out of the three study sites the Taav 1.3 site stands out as an exception in many ways. First of all, compared to the two other cores the Taav 1.3 site has remained generally much drier, with reconstructed water tables ranging from ~25 to ~55 cm when the range for the other two cores is from ~5 to ~35 cm. It is interesting that geographically Taav 1.3 is located in a higher altitude than the other sampling plots (661m vs. 554m and 349m). Consequently, it could be cautiously speculated that the peatland is further in its succession, with a thicker peat column, thus being more ombrotrophic. Dry ombrotrophic peatlands are more resilient to changes in moisture levels, whereas wetter peatlands can withstand only small perturbations in water tables. The age-depth model also indicates that the accumulation has remained more stable when compared with the other sites (Fig. 11-13), this unfers the peatland is closer to its climax phase. Many of the taxa recorded at this site (*Cyclopyxis arcelloides* type, *Difflugia pulex, Pseudodifflugia fulva* type), are taxa with wide water table optimas, or taxa that are known to be able to survive in relatively low moisture conditions (e.g. Charman et al. 2007, Mitchell et al. 2008, Zhang et al. 2017). It is thus also possible that in some cases the Taav 1.3 site experienced the same changes as the other two sites, but the changes were delayed and more minor due to the higher resilience of the system. For instance, the Taav 1.3 site shows a wet trend from 1833 AD to 1872 AD, which is 100-200 years later than in the Taav 2.2 and Abi 2.2 sites. Similarly, the wet peak experienced at 1986 AD could be caused by a delayed response to a potential mid 20th-century cooling (e.g. Overland et al. 2004, Serreze & Francis 2006) recorded in the Abi 2.2 site at 1953 AD.

Another viable explanation to the differences between the sites is that water table fluctuations are not necessarily always regulated by climate (Gunnarsson et al. 2002). A change in species composition can simply result from surface dynamics caused by the internal variability of the system (Payette 1988). Other autogenic factors such as fires cannot be ruled out either: especially after prolonged dry periods surface fires may cause abrupt wet shifts towards a shallower water table (Tuittila et al. 2007), such as in the Taav 1.3 core 1986 AD segment. However, charcoal particles were not detected, so a fire is in this case unlikely. Results of this thesis show that site-specific variation and potential random events complicate the construction of a consistent sub-regional scale peatland-climate linkage.

The recent drying trend depicted in both the Taav 2.2 and Abi 2.2 cores is also worth investigation. Both sites show rather unchanging post-LIA water table depths and species compositions indicate the sites have become drier. All three sites however show an abrupt present-day (2017 AD) composition

change, although this change results in only a small change in the water table reconstructions caused by an increased abundance of wetter taxa: both Abi 2.2 and Taav 1.3 show a major increase in wet-intermediate taxa *Archerella flavum,* and in Taav 2.2 this change appears to be caused by the intermediate *Nebela tincta* type. The slow drying and sudden abrupt wet change in all three sites can be attributed either as seasonal year-to-year variation, or a potential warning sign predicting a major future perturbation in water table depths. Swindles et al. (2015a) proposed that as permafrost peatlands thaw, the peatlands go through a gradual process of drying, increased aerobic decomposition and evaporation due to lowering water tables, and finally a melt and a collapse of permafrost domes, followed by soil saturated by the thaw water. Previous studies such as Åkerman & Johansson 2008 and Swindles et al. 2015a indicate that the peatlands in Northern Sweden have experienced significant permafrost thaw during the past few decades, and permafrost thaw is expected to increase further in the future (Luoto & Seppälä 2002, Schuur et al. 2008). Based on the long-term trends all three sites have gone through a long dry period potentially caused by increased evapotransporation linked to warming climate, and the abrupt change in species composition may be caused by permafrost thaw affecting the hydrology of the peatland. In all sites visited during the data collection permafrost potential ongoing warming-driven dessication was observed via visible cracking of permafrost domes. Thus, it is possible that the sites are approaching a threshold after which the peatland hydrology is controlled by the surrounding catchment area instead of precipitation (Swindles et al. 2015a). Considering that the amount of permafrost is expected to be reduced by at least 25% in the future (Canadell et al. 2007), these peatlands have the potential to transform into arctic fens which release carbon into the atmosphere and act as accelerating contributors to climate change (Lai 2009).

4.3. Sources of error

Potential error sources begin from the sampling itself, which is susceptible to sampling errors. Sample smearing in the coring process is common and may result in the mixing of different layers (Swindles et al. 2015a), which in the worst case could lead to inconsistencies in the dating results.

Dating errors can also occur due to natural sources. Several processes can affect the carbon available for ^{14}C analysis, which may lead to distortions between the measured date and the real event date. Chronologies might be interrupted by frost heaving, which may lead to the burial of surface peat with

older deposits. Sometimes peat samples may also be contaminated by younger carbon through the penetration of roots, infiltration of dissolved, modern organic carbon or bacteria affecting stored samples, which may lead to underestimates in bulk peat age (Merritt et al. 2004). Thawing of permafrost may also lead to a process called cryoturbation, in which the freezing of water during fall and winter season causes a greater volume of soil to be occupied, and the spring melt in turn causes the reverse effect, potentially moving organic carbon from the surface to deeper layers (Walker et al. 2008).

Similarly, as in the case of radiocarbon dating, past disturbances to the peat profile by physical effects such as trampling and biological activity may difficult the construction of a continuous chronology (Merritt et al. 2004). Since it is impossible to know what events have affected these discrepancies, it is important to combine both the lead and radiocarbon data to increase the reliability of the results. However, combining radiocarbon and lead dating results can itself cause chronological error, since the programs aim to extrapolate the gaps between the two different results (Loisel & Garneau 2010.)

The sample resolution of 2 cm results in the risk of some short-term changes remaining unnoticed. This risk increases especially during periods of rapid accumulation, which can result in a time gap of several centuries between samples. The accurate date of the samples may also differ due to possible errors in the sampling process. Although samples are handled with extreme care, accidents do happen, including the spill of the Taav 1.3 sample during the lead dating process, and the double injection of polonium in the Abi 2.2 sample. To minimize effects caused by human error, it is important to report every accident and adjust the results accordingly, while taking special caution when analyzing the results. An interesting factor that may also have affected the results is the size of the sieve, since the 300 / 180 µm size prevented larger taxa from being collected into the samples.

The largest potential error source involves the identification and analysis of testate amoebae results. I had no personal experience from testate amoebae prior to this thesis, which is why especially the samples analyzed first may suffer from identification errors. Some samples in this thesis included both wet and dry taxa. As mentioned in the earlier chapter, this is not necessarily problematic, since some dry taxa can indeed survive in wetter environments (Charman et al. 2007). One possible explanation for this discrepancy also is that some species have been identified incorrectly. Payne et al. (2011) noted that identification error can drastically alter predicted values especially in the case

of the taxon being abundant, causing unreliable reconstructions that poorly represent the realistic situation. Especially *Difflugia* are difficult to identify to the species level, and similar-looking *D. lucida* and *D. pristis* exist on variable parts of the hydrological gradient. Misidentifying one as the other could easily lead to this inconsistency. *Cyclopyxis arcelloides* is also a commonly misidentified taxon and extra caution should be applied when analyzing segments where it is abundant. In the case of there being doubt of whether a taxon is properly identified, it is safest to exclude the taxon entirely to avoid failures in reconstructions (Payne et al. 2011).

Another factor affecting accuracy of the results is the inability to reach count of 100 individuals, which may lead to the counted individuals representing only a fragment of the actual population. This was the case especially with the Taav 1.3 core, as from 15 cm downwards as only 50 specimens were counted instead of the suggested 100 due to high decomposition levels. Whether the conditions before 1833 AD in the aforementioned core are realistically depicted is thus disputable.

It is notable that past data on arctic testate amoebae assemblages is scarce (Zhang et al. 2017 & 2018), and to this day only one consecutive subarctic dataset has been collected, from the Abisko region (Swindles et al. 2015b) – thus the ecological response of these species in these environments is not very well known. Especially *Difflugia pulex* is considered a poorly modelled taxon (Amesbury et al. 2013). Testate amoebae data interpretation is complicated by the possible vertical movements in peat, which may result from frost heave or land subsidence caused by frost thaw. Land subsidence increases the moisture in soil, whereas frost heave shallows the active layer and decreases soil moisture, which elevates the water table. Together these two phenomena complicate predicting the mean water table surface (Kokfelt et al. 2009). However, in our case the peat cores showed no visible signs of cryoturbation, so this error is unlikely.

Finally, the transfer functions themselves are subject to error especially in the case of poorly known species ecology (Charman et al. 2007), the high dominance of a single taxa, or the simultaneous appearance of species with conflicting water table optimas (Amesbury et al. 2013). Charman et al. (2007) and Swindles et al. (2009) also found that testate amoebae transfer functions have poor performance in the drier end of water table depth, causing reconstructed water table values to overestimate actual values. This could have especially affected the drier Taav 1.3 core. In all cases the reconstructions seem to be largely driven by a few dominant taxa, for instance in the case of Abi

2.2, where the large abundance of *Pseudodifflugia fascicularis* appears to overrule the influence of dry taxa in the deeper layers. Thus, the results should be interpreted paying attention to both the trends depicted by the water table reconstruction and the actual species composition.

Despite the large amount of potential error sources, the results can be considered fairly trustworthy, since I paid extra caution to errors when interpreting the results, and I was constantly helped by professionals throughout the process.

5. Conclusions

The use of testate amoebae allowed me to model moisture dynamics for three subarctic permafrost peatlands in northern Sweden. Together with dating results I was able to reconstruct a chronology of modelled water tables ranging from the Dark Age Cold Period to the post-industrial warming, with a special focus on the past 320 years.

Table 5. Compilation of results, depicting whether the site has been wetter or drier than average during a climatic phase. Swindles Abi data refers to Swindles (2015a).

Climatic Phase	Site			
	Taav 1.3	**Taav 2.2**	**Abi 2.2**	**Swindles Abi**
DACP	Fluctuating	Fluctuating	No data	No data
MCA	Wetter	Drier	No data	No data
LIA	Drier	Wetter	Wetter	Wetter
PIW	Wetter	Drier	Drier	Drier

According to my hypotheses testate amoebae act as indicators of moisture levels in peatlands, allowing the reconstruction of past climatic events. The data from all three cores showed that the testate amoebae compositions have indeed changed throughout time, sometimes very abruptly within a short time frame. A majority of my results were supported by past studies and climatic data of the Holocene, identifying the Dark Age Cold period as variable, the Medieval Climate Anomaly as a dry period before the wetter Little Ice Age, and the post-industrial warming as a dry period. Out of the three cores the Taav 2.2 core matched with known climate history best, whereas the Taav 1.3 core provided opposite results. As the site was more ombrotrophic than the two other sites it is possible that the species composition is more resilient to change and thus less coupled with the climate. The

Abisko data also supported past studies, although the water table reconstructions for the site were complicated by the simultaneous appearance of wet and dry taxa, raising the question whether some taxa were falsely identified or if the reconstructions truly represented the actual conditions in this coring site.

The data also suggests that the post-industrial warming is different from previous climate phases. During the past there has been a link between cold periods and wet taxa, and similarly warm periods and dry taxa. It appears that the recent trend may be the opposite, with wet taxa increasing as the climate warms, potentially induced by rapid permafrost melt. This indicates that the scale of the post-industrial warming is different to that of the others and is causing widespread permafrost thaw and changes in precipitation patterns that are unprecedented during the Holocene period. During previous warm periods the increase in temperature has happened moderately on the course of centuries, during which species and ecosystems have had more time to adapt. Meanwhile, the current change is taking place on a scale of decades and has the potential to lead into major changes in sensitive ecosystems such as the Arctic area.

All in all, my results indicate that the moisture dynamics in permafrost peatlands are a complicated process, and variability in species composition and moisture dynamics can be large even in a local scale, such as with the contradicting Taavavuoma cores. This supports past studies that have indicated that peatlands are not only affected by external processes such as the climate, but also internal dynamics of the system.

My thesis results are largely supported by previous studies, which adds credibility to the data. However, in oder to draw further and more in-depth conclusions of ongoing changes in permafrost peatlands the use of a multi-proxy approach is essential.

6. Acknowledgements

models, the A.E Lalonde AMS Laboratory at the Canadian centre for AMS and environmental radionuclide research, and the University of Exeter in lending their faculties for lead dating.

7. References

Amesbury M. J., Swindels G. T., Bobrov A., Charman D. J., Holden J., Lamentowicz M., Mallon G., Mazei Y., Mitchell E. A. D., Payne R. J., Roland T. P., Turner T. E. & Warner B. G. (2016): Development of a new pan-European testate amoeba transfer function for reconstructing peatland palaeohydrology. Quaternary Science Reviews, 152(15): 132-151.

Appleby P. G & Oldfield F. (1978): The calculation of lead-210 dates assuming a constant rate of supply of unsupported 210Pb to the sediment. Catena, 5(1): 1-8.

Belyea L. R & Clymo R. S. (1999): Feedback control of the rate of peat formation. Biological Sciences, 268(1473): 1315-1321.

Blaauw M. & Christen A. (2011): Flexible Paleoclimate Age-Depth Models Using an Autoregressive Gamma Process. Bayesian Analysis, 6(3): 457-474.

Booth R. K, Lamentowicz M. & Charman D. J. (2010): Preparation and analysis of testate amoebae in peatland palaeoenrivonmental studies. Mires & Peat, 7: 1-7.

Boucher O., Friedlingstein P., Collins B. & Shine K. P. (2009): The indirect global warming potential and global temperature change potential due to methane oxidation. Environmental Research Letters 4(4): 044007.

Borge A. F., Westermann S., Solheim I. & Etzelmüller B. (2017): Strong degradation of palsas and peat plateaus in northern Norway during the last 60 years. The Cryosphere, 11: 1-16.

Broecker W. S. (2001): Was the Medieval Warm Period Global? Science, 291(5508): 1497-1499.

Brown J., Ferrians O. J., Heginbottom J. A. & Melnikov E. S. (1997): Circum-Arctic map of permafrost and ground-ice conditions.

Camill P. (2005): Permafrost Thaw Accelerates in Boreal Peatlands During Late-20th Century Climate Warming. Climatic Change, 68(1-2): 135-152.

Canadell J. G., Pataki D. E. & Pitelka L. F. (2007): Terrestrial Ecosystems in a Changing World. Springer.

Clymo R. S. (1984): The limits to peat bog growth. Philosophical transactions of the royal society of London, 303: 605-654.

Clymo R. S., Oldfield F., Appleby P. G., Pearson G. W., Rat-nessar P. & Richardson N. (1990): A record of atmospheric deposition in a rain-dependent peatland. Philosophical Transactions of the Royal Society of London B, 327: 331–338.

Charman D. J, Hendon D. & Woodland W. A. (2000): The identification of testate amoebae (Protozoa: Rhizopoda) in peats. QRA Technical Guide No. 9, Quaternary Research Association.

Charman D. J., Blundell A., Alm J., Bartlett S., Begeot C., Blaauw M., Chambers F., Daniell J., Evershed R., Hunt J., Karofeld E., Korhola A., Kuester H., Laine J., Magny M., Mauquoy D., McClymont E., Mitchell F., Oksanen P., Pancost R., Sarmaja-Korhonen K., Seppä H. & Sillasoo Ü. (2007): A new European testate amoebae transfer function for palaeohydrological reconstruction on ombrotrophic peatlands. Journal of Quaternary Science, 22(3): 209-221.

Collins M., Knutti R., Arblaster J., Dufresne J.-L., Fichefet T., Friedlingstein P., Gao X., Gutowski W.J., Johns T., Krinner G., Shongwe M., Tebaldi C., Weaver A.J. & Wehner M. (2013): Long-

term Climate Change: Projections, Commitments and Irreversibility. Climate Change 2013: The Physical Science Basis. Contribution of Working Group I to the Fifth Assessment Report of the Intergovernmental Panel on Climate Change. Cambridge University Press, Cambridge, United Kingdom and New York, NY, USA: 1055.

Cook B. I., Ault T. R. & Smerdon J. E. (2015): Unprecedented 21st century drought risk in the American Southwest and Central Plains. Sci. Adv., 1: e1400082 De

Fisher R. E, Sriskantharajah S., Lowry D., Lanoisellé M., Fowler C. M. R., James R. H., Hermansen O., Lund Myhre C., Stohl A., Greinert J., Nisbet-Jones P. B. R., Mienert J. & Nisbet E. G. (2011): Arctic Methane Sources: Isotopic Evidence for Atmospheric Inputs. Atmospheric Science, 38(21).

Gallego-Sala A., Charman D. J., Brewer S., Page S. E., Prentice I. C., Friedlingstein P., Moreton S., Amesbury M. J., Beilman D. W., Björck S., Blyakharchuk T., Bochicchio C., Booth R. K., Bunbury J., Camill P., Carless D., Chimner R. A., Clifford M., Cressey E., Courtney-Mustaphi C., De Vleeschouwer F., de Jong R., Fialkiewicz-Koziel B., Finkelstein S. A., Garneau M., Githumbi E., Hribjlan J., Holmquist J., Hughes P. D. M., Jones C., Jones M. C., Karofeld E., Klein E. S., Kokfelt U., Korhola A., Lacourse T., Le Roux G., Lamentowicz M., Large D., Lavoie M., Loisel J., Mackay H., MacDonald G. M., Makila M., Magnan G., Marchant R., Marcisz K., Cortizas A. M., Massa C., Mathijssen P., Mauquoy D., Mighall T., Mitchell F. J. G., Moss P., Nichols J., Oksanen P. O., Orme L., Packalen M. S., Robinson S., Roland T. P., Sanderson N. K., Sannel A. B. K., Silva-Sánchez N., Steinberg N., Swindles G. T., Turner T. E., Uglow J., Väliranta M., van Bellen S., van der Linden M., van Geel B., Wang G., Yu Z., Zaragoza-Castells J., Zhao Y. (2018): Latitudinal limits to the predicted increase of the peatland carbon sink with warming. Nature Climate Change 8(10): 907.

Garcia J. L., Patel B. K. C. & Ollivier B. (2000): Taxonomic, phylogenetic, and ecological diversity of methanogenic Archaea. Anaerobe, 6(4): 205–226.

Godwin H. (1962): Radiocarbon dating. Nature, 195: 943–945

Gunnarsson U., Malmer N. & Rydin, H. (2002): Dynamics or constancy in Sphagnum dominated mire ecosystems? A 40-year study. Ecography, 25: 685–704.

Helama S., Jones, P. D. & Briffa K. R. (2017): Dark Ages Cold Period: A literature review and directions for future research, Holocene, 27: 1600–1606.

Holmquist J. R., Booth R. K. & MacDonald G. M. (2016): Boreal peatland water table depth and carbon accumulation during the Holocene thermal maximum, Roman Warm Period, and Medieval Climate Anomaly. Palaeogeography, Palaeoclimatology, Palaeoecology, 444: 15-27.

Hugelius G., Strauss J., Zubrzycki S., Harden J. W., Schuur E. A. G., Ping C.-L., Schirrmeister L., Grosse G., Michaelson G. J., Koven C. D., O'Donnell J. A., Elberling B., Mishra U., Camill P., Yu Z., Palmtag J. & Kuhry P. (2014): Estimated stocks of circumpolar permafrost carbon with quantified uncertainty ranges and identified data gaps. Biogeosciences, 11(23): 6573-6593.

Hughes P. D. M., Mauquoy D., Barber K. E. & Langdon, P. G. (2000): Mire-development pathways and palaeoclimatic records from afull Holocene peat archive at Walton Moss, Cumbria, England. The Holocene, 10: 465–79.

Ingram H. A. P. (1978): Soil layers in mires: function and terminology. Journal of Soil Science, 29(2): 224-227.

IPCC, 2018: Global warming of 1.5°C. An IPCC Special Report on the impacts of global warming of 1.5° above pre-industrial levels and related global greenhouse gas emission pathways, in the context of strengthening the global response to the threat of climate change, sustainable development, and efforts to eradicate poverty [V. Masson-Delmotte, P. Zhai, H. O. Pörtner, D. Roberts, J. Skea, P.R. Shukla, A. Pirani, W. Moufouma-Okia, C. Péan, R. Pidcock, S. Connors,

J. B. R. Matthews, Y. Chen, X. Zhou, M. I. Gomis, E. Lonnoy, T. Maycock, M. Tignor, T. Waterfield (eds.)]. In Press.

Jassey V. E. J., Meyer C., Dupyu C., Bernard N., Mitchell E. A. D., Touissant M.-L., Metian M., Chatelain A. P. & Gilbert D. (2013): To What Extent Do Food Preferences Explain the Trophic Position of Heterotrophic and Mixotrophic Microbial Consumers in a *Sphagnum* Peatland? Microbial Ecology, 66(3): 571-580.

Jassey V. E. J., Signarbieux C., Hättenschwiler S., Bragazza L., Buttler A., Delarue F., Fournier D., Laggoun-Dénfarge F., Lara E., Mills R. T. E., Mitchell E. A. D., Payne R. J. & Robroek B. J. M. (2015): An unexpected role for mixotrophs in the response of peatland carbon cycling to climate warming. Scientific Reports, 5: 16931.

Kilpisjärvi Biological Station, weather data 1981-2010. Visited 7/18. http://www.helsinki.fi/kilpis/Ilmasto/tunnuslukuja.htm

Kokfelt U., Rosén P., Schoning K., Christensen T. R., Förster J., Karlsson J., Reuss N., Rundgren M., Callaghan T. V., Jonasson C. & Hammarlund D. (2009): Ecosystem responses to increased precipitation and permafrost decay in subarctic Sweden inferred from peat and lake sediments. Global Change Biology, 15(7): 1652-1663.

Korhola A., Ruppel M., Seppä H., Väliranta M., Virtanen T. & Weckström J. (2010): The importance of northern peatland expansion to the late-Holocene rise of atmospheric methane. Quaternary Science Reviews xxx: 1-7.

Lai D. Y. F. (2009): Methane Dynamics in Northern Peatlands: A Review. Pedosphere, 19(4): 409-421.

Lamarre A., Garneau M. & Ansong H. (2012): Holocene paleohydrological reconstruction and carbon accumulation of a permafrost peatland using testate amoeba and macrofossil analyses, Kuujjuarapik, subarctic Québec, Canada. Review of Paleobotany and Palynology 186: 131-141.

Lamentowicz M., Mueller M., Galka M., Barabach J., Milecka K., Goslar T. & Binkowski M. (2015): Reconstructing human impact on peatland development during the past 200 years in CE Europe through biotic proxies and X-ray tomography. Quaternary International, 357.

Langdon P. G. & Barber K. E. (2005): The climate of Scotland over the last 5000 years inferred from multiproxy peatland records: intersite correlations and regional variability. Journal of Quaternary Science, 20: 549–66.

Lara M. J., McGuire A. D., Euskirschen E. S., Tweedie C. E., Hinkel K. M., Skurikhin A. N., Romanovsky V. E., Grosse G., Bolton W. R. & Genet H. (2015): Polygonal tundra geomorphological change in response to warming alters future CO2 and CH4 flux on the Barrow Peninsula. Global Change Biology, 21(4): 1634-51.

Le Roux G. & Marshall W. A. (2011): Constructing recent peat accumulation chronologies using atmospheric fall-out radionuclides. Mires and Peat, 7(8).

Linderholm, H., Nicolle, M., Francus, P., Gajewski, K. Helama, S., Korhola, A., Solomina, O., Yu, Z., Zhang, P., D'Andrea, W.J., Debret, M., Divine, D., Gunnarson, B.E., Loader, N.J., Massei, N., Seftifgen, K., Thomas, E.K., Werner, J., Andersson, S., Berntsson, A., Luoto, T.P., Nevalainen, L. Saarni, S., Väliranta. M. (2018): Arctic hydroclimate variability during the last 2000 years – current understanding and research challenges. Climate of the Past, 14: 473–514.

Ljungqvist F. C. (2010): A new reconstruction of temperature variability in the extra-tropical northern hemisphere during the last two millennia. Geografiska Annaler, Series A: Physical Geography, 92(3): 339-351.

Loisel J. & Garneau M. (2010): Late Holocene paleoecohydrology and carbon accumulation estimates from two boreal peat bogs in eastern Canada: Potential and limits of multi-proxy archives. Palaeogeography, Palaeoclimatology, Palaeoecology, 291: 493-533.

Loisel J., Yu Z., Beilman D. W., Camill P., Alm J., Amesbury M. J., Anderson D., Andersson S., Bochicchio C., Barber K., Belyea L. R., Bunbury J., Chambers F. M., Charman D. J., Vleeschouwer F. de, Fiałkiewicz-Kozieł B., Finkelstein S. A., Gałka M., Garneau M., Hammarlund D., Hinchcliffe W., Holmquist J., Hughes P., Jones M. C., Klein E. S., Kokfelt U., Korhola A., Kuhry P., Lamarre A., Lamentowicz M., Large D., Lavoie M., MacDonald G., Magnan G., Mäkilä M., Mallon G., Mathijssen P., Mauquoy D., McCarroll J., Moore T. R., Nichols J., O'Reilly B., Oksanen P., Packalen M., Peteet D., Richard P. JH., Robinson S., Ronkainen T., Rundgren M., Sannel A. B. K., Tarnocai C., Thom T., Tuittila E-S., Turetsky M., Väliranta M., Linden M. van der., Geel B. van., Bellen S. van., Vitt D., Zhao Y. & Zhou W. (2014): A database and synthesis of northern peatland soil properties and Holocene carbon and nitrogen accumulation. The Holocene, 24: 1028– 1042.

Luoto M. & Seppälä M. (2002): Modelling the distribution of palsas in Finnish Lapland with logistic regression and GIS. Permafrost and Periglacial Processes, 13(1): 17-28.

Mauquoy D., Geel B. van., Blaauw M., Speranza A. & Plicht J. van der. (2004): Changes in solar activity and Holocene climatic shifts derived from 14C wiggle-match dated peat deposits. The Holocene, 14(1): 45-52.

Mayewski P. A., Rohling E. E., Stager J. C., Karlén W., Maasch K. A., Meeker L. D., Meyerson E. A., Gasse F., Kreveld S. van., Holmgren K., Lee-Thorp J., Rosqvist G., Rack F., Staubwasser M., Schneider R. R. & Steig E. J. (2004): Holocene climate variability. Quaternary Research, 62(3): 243-255.

Merritt R. T., Manning S. W. & Wieder R. K. (2004): Dating recent peat deposits. Wetlands, 24(2): 324-356.

Mitchell E. A. D, Charman D. J & Warner B. G. (2008): Testate amoebae analysis in ecological and paleoecological studies of wetlands: past, present and future. Biodiversity Conservation, 17: 2115.

Moore P.D. (1987): Ecological and hydrological aspects of peat formation. Geological Society London, Special Publications, 32: 7-15.

Moore T. R. & Knowles R. (1989): The influence of water table levels on methane and carbon dioxide emissions from peatland soils. Canadian Journal of Soil Science, 69(1): 33-38.

Oksanen P. O. & Väliranta M. (2006): Palsasuot muuttuvassa ilmastossa (Palsa mires in a changing climate). Suo, Mires and peat, 57(2): 33-43.

Olefeldt D. & Roulet N. (2012): Effects of permafrost and hydrology on the composition and transport of dissolved organic carbon (DOC) in a subarctic peatland complex. Journal of Geophysical Research Atmospheres, 117.

Overland J. E., Spillane M. C., Percival D. B., Wang M. & Mofjeld H. O. (2004): Seasonal and regional variation of pan-Arctic surface air temperature over the instrumental record. Journal of Climate, 17(14): 3263-3282.

Payette S. (1988): Late-Holocene Development of Subarctic Ombrotrophic Peatlands: Allogenic and Autogenic Succession. Ecology, 69(2): 516-531.

Payne R. J. & Mitchell E. A. D. (2009): How many is enough? Determining optimal count totals for ecological and palaeoecological studies of testate amoebae. Journal of Paleolimnology 42(4).

Payne R. J., Lamentowicz M. & Mitchell E. A. D. (2011): The perils of taxonomix inconsistency in quantitative palaeoecology: experiments with testate amoebae data. Boreas, 40: 15-27.

Reimer P. J., Bard E., Bayliss A., Beck J. W., Blackwell P. G., Bronk Ramsey C., Buck C. E., Edwards R. L., Friedrich M., Grootes P. M., Guilderson T. P., Haflidason H., Hajdas I., Hatté C., Heaton T. J., Hoffmann D. L., Hogg A. G., Hughen K. A., Kaiser K. F., Kromer B., Manning S. W., Niu M., Reimer R. W., Richards D. A., Scott M. E., Southon J. R., Turney C. S. M. &

van der Plicht J. (2013): IntCal13 and Marine13 radiocarbon age calibration curves 0-50,000 yr cal BP. Radiocarbon, 55(4): 1869-1887.

Renssen H., Seppä H., Heiri O., Roche D. M., Goosse H., Fichefet T. (2009): The spatial and temporal complexity of the Holocene thermal maximum. Nature Geoscience, 2: 411–414.

Renssen H., Seppä H., Crosta X., Goosse H. & Roche D. M. (2012): Global characterization of the Holocene Thermal Maximum. Quaternary Science Reviews, 48: 7-19.

Ribes J. C. & Nesme-Ribes E. (1993): The solar sunspot cycle in the Maunder minimum AD1645 to AD1715. Astronomy and Astrophysics, 276: 549–563.

Schuur E. A. G., Bockheim J., Canadell J. G., Euskirchen E., Field C. B., Goryachkin S. V., Hagemann S., Kuhry P., Lafleur P. M., Lee H., Mazhitova G., Nelson F. E., Rinke A., Romanovsky V. E, Shiklomanov N., Tarnocai C., Venevsky S., Vogel J. G. & Zimov S. A. (2008): Vulnerability of Permafrost Carbon to Climate Change: Implications for the Global Carbon Cycle. BioScience, 58(8): 701–714.

Screen J. A & Simmons I. (2010): The central role of diminishing sea ice in recent Arctic temperature amplification. Nature, 464: 1334-1337.

Seppälä M. (1997): Distribution of permafrost in Finland. Bull. Geological Society Finland, 69(1-2): 87-96

Serreze M. C & Francis J. A. (2006): The Arctic Amplification Debate. Climatic Change, 76(3-4): 241-246.

Siegel D. I. (1988): Evaluating cumulative effects of disturbance on the hydrologic function of bogs, fens and mires. Environmental Management, 12(5): 621-626.

Stuiver M. & Reimer P. J. (1993): Extended 14C Data Base and Revised Calib 3.0 14C Age Calibration Program. Radiocarbon, 35: 215-230.

Sullivan M. & Booth R. (2007): Key to testate amoebae inhibiting *Sphagnum*-dominated peatlands with an emphasis on taxa preserved in Holocene sediments. Working draft – 21 March 2007. Earth & Environmental Science Department, Lehigh University.

Swindles G. T., Morris P.J., Watson E. J., Turner T. E., Roland T. P., Amesbury M. J., Kokfelt U., Schoning K., Pratte S., Gallego-Sala A., Charman D. J., Sanderson N., Garneau M., Carrivick J. L., Woulds C., Holden J., Parry L. & Galloway J. M. (2015a): The long-term fate of permafrost peatlands under rapid climate warming. Scientific Reports, 5: 17951.

Swindles G. T., Amesbury M. J., Turner T. E., Carrivick J. L., Woulds C., Raby C., Mullan D., Roland T. P., Galloway J. M., Parry L., Kokfelt U., Garneau M., Charman D. J & Holden J. (2015b): Evaluating the use of testate amoebae for palaeohydrological reconstruction in permafrost peatlands. Palaeogeography, Palaeoclimatology, Palaeoecology, 424: 111-122.

Swindles G. T., Holden J., Raby C., Turner T. E., Blundell A., Charman D. J., Menberu M. & Klöve B. (2015c): Testing peatland water-table depth transfer functions using high-resolution hydrological monitoring data. Quaternary Science Reviews, 120: 107-117.

Tarnocai C., Canadell J. G., Schuur E. A. G., Kuhry P., Mazhitova G. & Zimov S. (2009): Soil organic carbon pools in the northern circumpolar permafrost region. Global Biogeochemical Cycles, 23(2).

ter Braak C. J. F & Juggins S. (1993): Weighted averaging partial least squares regression (WA-PLS): an improved method for reconstructing environmental variables from species assemblages. Hydrobiologia, 269(1): 485-502.

Tolonen K., Warner B. G. & Vasander H. (1992): Ecology of Testaceans (Protozoa: Rhizopoda) in Mires in Southern Finland: I. Autecology. Archiv für Protistenkunde, 142: 119-138.

Tuittila E-S., Väliranta M., Laine A. & Korhola A. (2007): Quantifying patterns and controls of mire vegetation succession in a southern boreal bog using a combination of partial ordinations. Journal of Vegetation Science in press.

Treat C. C. & Jones, M. C. (2018): Near-surface permafrost aggradation in Northern Hemisphere peatlands shows regional and global trends during the past 6000 years. The Holocene, 28(6): 998 –1010.

Turetsky M. R., Wieder R. K, Williams C. J. & Vitt D. H. (2000): Organic matter accumulation, peat chemistry, and permafrost melting in peatlands of boreal Alberta. Écoscience, 7(3): 115-122.

Turunen J., Tomppo E., Tolonen K. & Reinikainen A. (2002): Estimating carbon accumulation rates of undrained mires in Finland-application to boreal and subarctic regions. The Holocene, 12: 69-80.

Väliranta M., Korhola A., Seppä H., Tuittila E.-S., Sarjama-Korjonen K., Laine J. & Alm J. (2007): High-resolution reconstruction of wetness dynamics in a southern boreal raised bog, Finland, during the late Holocene: a quantitative approach. The Holocene, 17(8): 1093-1107.

Väliranta M., Blundell A., Charman D. J., Karofeld E., Korhola A., Sillasoo Ü. & Tuittila E.-S. (2012): Reconstructing peatland water tables using transfer functions for plant microfossils and testate amoebae: A methodological comparison. Quaternary International, 268(34-43).

Walker D. A., Epstein H. E., Romanovsky V. E., Ping C. L., Michaelson G. J., Daanen R. P., Shur Y., Peterson R. A., Krantz W. B., Raynolds M. K., Gould W. A., Gonzales G., Nicolsky D. J., Vonlanthen C. M., Kade A. N., Kuss P., Kelley A. M., Munger C. A., Tarnocai C. T., Matveyeva N. V & Daniëls F. J. A. (2008): Arctic patterned-ground ecosystems: A synthesis of field studies and models along a North American Arctic Transect. Journal of Geophysical Research, 113(G3).

Wanner H., Beer J., Bütikofer J., Crowley T. J., Cubash U., Flückiger J., Goosse H., Grosjean M., Joos F., Kaplan J. O., Küttel M., Müller S. A., Prentice I. C., Solomina O., Stocker T. F., Tarasov P., Wagner M. & Widmann M. (2008): Mid- to late Holocene climate change: an overview. Quaternary Science Reviews, 27(19-20): 1791-1828.

Wanner H., Solomina O., Grosjean M., Ritz S. P. & Jetel M. (2011): Structure and origin of Holocene cold events. Quaternary Science Reviews, 30(21-22): 3109-3123.

Warner B. G. (1990): Testate Amoebae (Protozoa). Methods in Quaternary ecology, vol. Reprint Series 5. Geoscience Canada, St. John's, Newfoundland: 65–74

Woodland W. A., Charman D. J. & Sims P. C. (1998): Quantitative estimates of water tables and soil moisture in Holocene peatlands from testate amoebae. The Holocene, 8(3): 261-273.

Wu J. & Roulet N. T. (2014): Climate change reduces the capacity of northern peatlands to absorb the atmospheric carbon dioxide: The different responses of bogs and fens. Global Biochemical Cycles, 28(10): 1005-1024.

Yu Z., Loisel J., Brosseau D., Beilman D. & Hunt S. (2010): Global peatland dynamics since the Last Glacial Maximum. Geophysical Research letters, 37.

Zhang H., Amesbury M. J., Ronkainen T., Charman D. J., Gallego-Sala A. V. & Väliranta M. (2017): Testate amoeba as palaeohydrological indicators in the permafrost peatlands of north-east European Russia and Finnish Lapland. Journal of Quaternary Science, 32(7): 976-988.

Zhang H., Väliranta M., Amesbury M. J., Charman D. J., Laine A. & Tuittila E.-S. (2018): Successional change of testate amoeba assemblages along a space-for-time sequence of peatland development. European Journal of Protistology, 66: 36-47.

Zhang T. (2005): Influence of the seasonal snow cover on the ground thermal regime: An overview. Reviews of Geophysics, 43(4).

Åkerman H. J. & Johansson M. (2008): Thawing permafrost and thicker active layers in subarctic Sweden. Permafrost and Periglacial Processes, 19: 279–292.